Renewable and Sustainable Energy Reviews 135 (2021) 110186

Contents lists available at ScienceDirect

Renewable and Sustainable Energy Reviews

journal homepage: http://www.elsevier.com/locate/rser

# A review of multiple input DC-DC converter topologies linked with hybrid electric vehicles and renewable energy systems

Azuka Affam *, Yonis M. Buswig, Al-Khalid Bin Hj Othman, Norhuzaimin Bin Julai, Ohirul Qays

*Department of Electrical and Electronic Engineering, Faculty of Engineering, Universiti Malaysia Sarawak, Kota Samarahan, Sarawak, 94300, Malaysia*

ARTICLE INFO

*Keywords:*
Multi-input dc-dc converter
Renewable energy system
Hybrid electric vehicle
Double input
Topology
Renewable energy
Review

ABSTRACT

In this paper, the contemporary development in multiple input dc-dc converters are identified and examined. The quest to mitigate the difficulties associated with employing renewables in distribution systems and electric vehicles (EVs) has yielded many new converter topologies. These new topologies have easier control, lower parts count, are cheaper and are worthy alternatives to the typical series or parallel connection of converters. The converters are identified by three divisions that bother on the isolation between the respective ports. The electrically connected converters do not have isolation between the ports, and thus, a dc link connects the ports. Electromagnetically connected converters use a dc-link to connect input ports, but the input ports and output port are isolated. In magnetically connected converters, input ports are separated by multiple winding transformer, just as the output port is isolated from the input ports by the winding. The formation, structure, characteristics, operation, merits and demerits of the converters will be presented. Thereafter, comparisons will be done based on the distinct features of the converters. This review identifies that converter properties depend on the specific application requirement and thus, no converter fulfills all demands in the industry. Prospective future research trends are suggested. This work aims to update on research done during the time gap since the last comprehensive reviews.

## 1. Introduction

Recent developments have seen an unprecedented increase in efforts targeted at promoting, developing and managing renewable energy (RE) sources. Reasons for these are not far-fetched. Conventional energy sources (fossil fuels) have been classified as agents of environmental pollution and degradation, global warming, and greenhouse effect. These are mainly caused by gases emitted by the burning of these fossil fuels. This gas emission has aggravated the demand by environmentalists for definite action to mitigate the effects of fossil fuels on the environment. This intent to reduce emissions has led to the inevitable employment of RE sources for power generation.

In the transportation sector, conventional motor vehicles also pose challenges of environmental pollution and global warming. Ecological data sources in the United States reveal that transport-related machinery accounts for more than a quarter of the global warming emission gases [1]. The advent of the hybrid electric vehicle (HEV) has come to the fore, aiming to ameliorate transportation induced gas emissions. In HEVs, the use of multiple energy sources has been targeted to reduce operation cost and increase vehicle efficiency. RE sources have been identified as free, clean, and having low long-term maintenance costs. Despite the advantages offered by RE sources over fossil fuels, the former face challenges that continue to limit their application. Three scenarios highlight the importance of multi-input converters. Firstly, most RE sources typically have been found to possess low output voltage. This peculiarity hinders their application in hybrid systems where there is need for high voltage at the inverter level. Secondly, the stochastic nature of some variable RE sources implies unpredictability and inconsistency in quantity, reliability, and availability in the process of power generation. Thirdly, there are limits to the slew rate of some sources and storage devices like the fuel cell, batteries, and supercapacitor.

A panacea to these challenges is the combination of two or more RE sources and has given birth to the multi-input DC-DC converter. The general structure of a multiple input converter has been illustrated in Fig. 1. In the structure, instead of individual energy sources having their specific DC-DC converter, the routing is such that, all the input sources are directed to a common converter. In this condition, control of the input and output variables is central thereby reducing cost.

Structurally, converters can be identified by their isolation type. They could be either be isolated converters or non-isolated converters [2]. Isolation employs a transformer winding to transfer energy to the

* Corresponding author.
*E-mail address:* 18010014@siswa.unimas.my (A. Affam).

https://doi.org/10.1016/j.rser.2020.110186
Received 16 January 2020; Received in revised form 28 July 2020; Accepted 29 July 2020
Available online 8 August 2020
1364-0321/

**List of abbreviations**

| | |
|---|---|
| AC | Alternating Current |
| DC | Direct Current |
| EV | Electric Vehicle |
| FC | Fuel Cell |
| FCBB | Forward-conducting bidirectional-blocking |
| HB | Half Bridge |
| HEV | Hybrid Electric Vehicle |
| kW | Kilowatt |
| LC | Inductor-capacitor |
| LLC | Inductor-inductor-capacitor |
| MIMO | Multi-input-multi-output |
| OFC | Output filter cell |
| PCSC | Pulsating current-source cells |
| PSC | Pulsating source cell |
| PV | Photovoltaic |
| PVSC | Pulsating voltage-source cell |
| PWM | Pulse Width Modulation |
| RE | Renewable Energy |
| SC | Switched Capacitor |
| SISO | Single-input-single-output |
| SPTT | Single-pole-triple-throw |
| UC | Ultracapacitor |
| VM | Voltage Multiplier |
| $V_{out}$ | Output Voltage |
| VTR | Voltage Transfer Ratio |
| ZCS | Zero Current Switching |
| ZVS | Zero Voltage Switching |
| ZVT | Zero Voltage Transition |

output stage from the input stage. The increased number of inputs result in a multi-winding transformer, which uses phase angle and inductance by dispersion to control the respective inputs. The voltage induced in the secondary winding is an aggregate of fluxes produced by individual primary windings. The application of multi-winding transformers provides galvanic isolation that reduces the probability of shock. There are also advantages of high voltage gain, voltage matching, reduced ratings for semiconductors' current/voltage, and good noise filtering. Unfortunately, the inclusion of transformer windings causes the converter designs to become difficult, bulky and more expensive. Besides, there are challenges associated with complex control requirements and high semiconductor count [3].

In non-isolated converters, the input stage and the output stage do not have isolation between them. Hence, they do not require a transformer winding. There is a common ground shared by the power ports. Some advantages of non-isolated multi-input converters are high power density, low cost, relatively easier control and smaller size [2].

This review paper aims to present the state-of-the-art for multi-input DC-DC converters in which RE sources are applied. Multi-input converters have been reviewed in several publications. Earlier reviews done, focused on the multi-input converters as applied in HEVs [1] and grid integration [2,4]. The review done in Ref. [5] covered the significant topologies at the time it was published (2015). However, the authors did not exhaustively scrutinise recently developed topologies. The review in Ref. [3] had covered up until 2016. There is a considerable time gap during which new topologies have been proposed. Thus, an up to date review is necessary to provide invaluable information to prospective researchers and designers. This paper builds majorly on the work done in Refs. [3,5]. In this work, the authors aim to present and analyse the current techniques for developing RE source based multi-input converters. The study focus is on converters capable of serving in HEV drive train and/or power generation for standalone or DC microgrids. Analyses of the converters are based on isolation, source utilisation, bidirectional operation, voltage gain and output port characteristics. The synthesis and utilisation of the multi-input converters as presented in this study, will advance power electronic designers and researchers' efforts to achieve optimally operating multi-input converters in HEVs and RE systems.

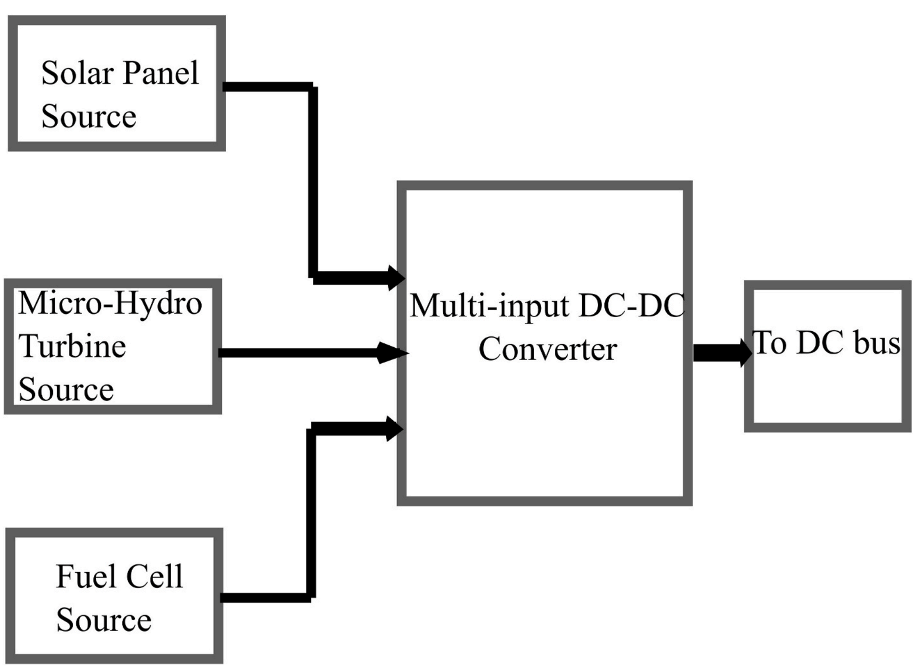


**Fig. 1.** A representation of unidirectional operation of multi-input DC-DC converter supplying a microgrid using RE sources.

## 2. Magnetically connected multi-input converters

The inadequacy of conventional isolated converter like the flyback and forward converters is stemmed in the fact that they are only suitable in low power requirements. In applications like RE generation and HEV, converters like these, cannot satisfy the medium or high voltage and power density requirements.

### 2.1. Multi-input converter with buck-boost configuration

Some of the earliest isolated multi-input converters [6] takes the form of a converter having a buck-boost configuration. The two functions of the isolating transformer are to act as an inductor for the converter and to produce aggregate fluxes for the respective input sources. This converter has three operating states. In the first state, switch, $S_1$ turns on, $S_2$ is off, and $V_1$ charges the inductor, $L$. The inverse occurs for the switches in the second state as $S_2$ is on, $S_1$ is off, and $V_2$ charges the inductor. During the first two modes, the load is serviced by the output capacitor as there is no transfer of power to the output stage from the input stage. In the third operating state, both switches are turned off, and neither $V_1$ nor $V_2$ charges the inductor. Thus, power is delivered by the inductor to the load. For this converter, the output voltage, $V_{out}$ is given as:

$$V_{out} = \frac{D_1}{N_1(1-D_1-D_2)}V_1 + \frac{D_2}{N_2(1-D_1-D_2)}V_2 \tag{1}$$

where $N_1$ and $N_2$ are the number of turns for the transformer input windings, $D_1$ and $D_2$ are the respective duty ratios of $S_1$ and $S_2$, and $V_1$ and $V_2$ represent the voltage of the respective input sources.

The initial converter used two DC sources as input. A significant weakness of this converter is the absence of optimal source utilisation. Simultaneous power delivery to the load by the two sources is not feasible. The forward conduction of the diodes limited this converter to unidirectional operation. However, the simple control technique implies that soft switching is absent. At very high frequency, hard switching result in device stress, electromagnetic interference and energy losses in stray inductor and capacitor. These losses impact negatively on the efficiency of the converter. Implementation of soft switching reduces the switching losses thereby improving the efficiency of the converter. With regards to control complexity, hard switching operation do not involve any extra control circuitry or auxiliary circuit. Soft switching involves auxiliary switching circuitry. Hence, the control of soft switched converters is more complex. In Ref. [7], the authors investigated the control and boundaries of stability for the converter. Proposed modifications in Ref. [8] combined a photovoltaic (PV) panel input and a commercial alternating current (AC) line. The ac line meant that a power factor corrector was included. The proposed topology in Ref. [9] added the battery recharge capacity and three input sources.

### 2.2. Multi-input full-bridge and half-bridge converter

The principle of flux additivity has been applied in Ref. [10] where dual current fed converters serve at the input, and a different full-bridge diode rectifier served at the output stage. The structure is shown in Fig. 2 and can accommodate numerous input sources. The converter operation is such that control is achieved by phase-shifted pulse width modulation (PWM) with the duty ratio of the switches at 0.5. The driving signals of complementary switches on each half bridge (HB) leg are phase shifted

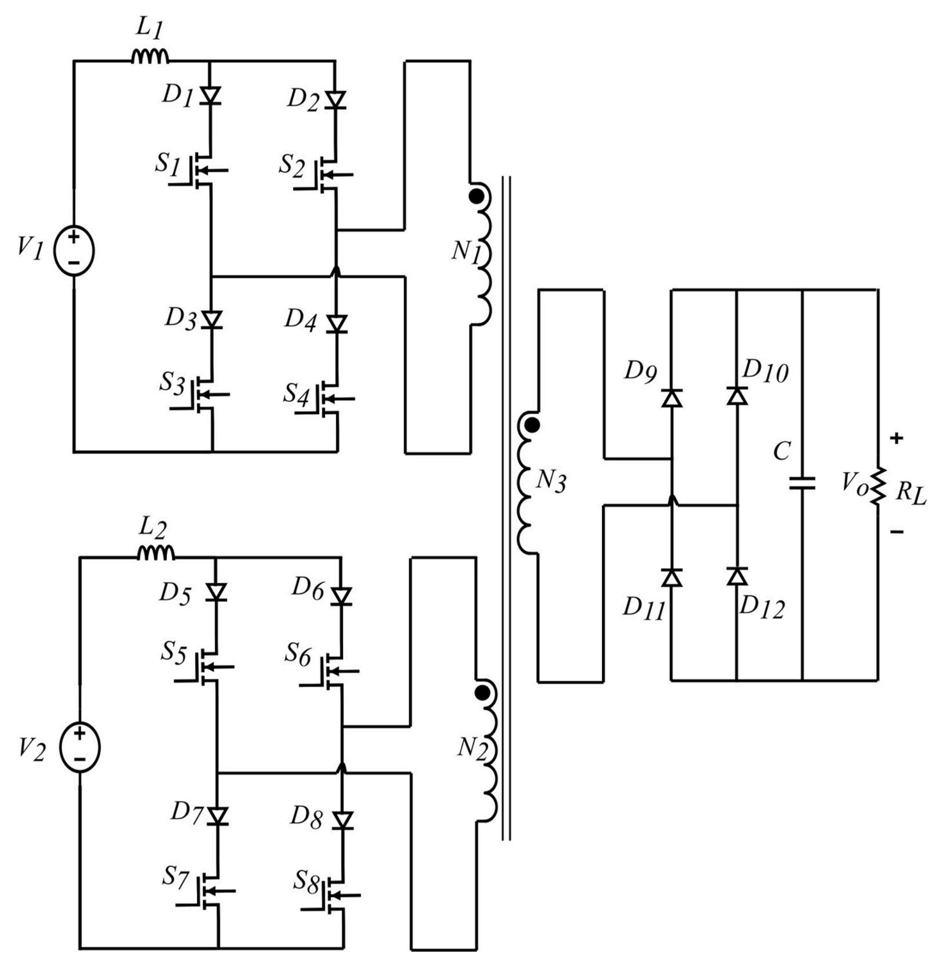


**Fig. 2.** Flux additivity based multi-input full bridge converter [10].

by 180°. At duty ratio other than 0.5, a current change will arise in the input inductor, thereby causing clamped zero-voltages in the windings. This will impede energy transfer from the primary winding to the secondary winding. The output voltage $V_O$ is:

$$V_O = \frac{N_3}{N_1}V_1 + \frac{N_2}{N_1}V_2 \tag{2}$$

$N_1$, $N_2$, and $N_3$ represent the number of turns for the transformer input windings, $V_1$ and $V_2$ are the voltages of the respective input sources.

Despite the presence of soft switching as an advantage, the absence of a bidirectional port poses a drawback in the event of grid applications when batteries or HEVs serve as input sources. The presence of soft switching is evident in the zero voltage switching (ZVS) and zero current switching (ZCS) operations of the converter. There is zero-loss transition when the switches turn on or off. Excess energy in the grid (output) cannot be channelled to other use (input). Modifications in Ref. [11] achieved bidirectional functionality by including a full bridge with an inductor in the output port. In this way, battery can be charged by a fuel cell (FC) or the output port voltage. In this work, the insertion of capacitors as connected to the high voltage side, reduces the fluctuation of the secondary winding voltage. A four-input converter was proposed based on the addition of windings and full-bridge rectifiers [12]. Four separate H-bridge input windings are applied to a high-frequency transformer in Ref. [13]. Suetomi et al., [14], attempted to better the soft-switching performance of the converter, by equipping the secondary side of the input converters with series resonance tank. This converter was also used to validate the theory that the increment of number of input sources improves efficiency of the converter. The operation of the two input circuits in the converter resulted in higher efficiency at lower duty ratio. In Ref. [15], optimised two input full bridge converters are presented. Yang et al. [16], proposed the double phase shift control strategy for the two-input isolated full bridge converter. A critical drawback of full-bridge converters is complex control system associated with steep numerical values of devices and driving technology [17].

Half-bridge topology principles have been extended to multi-input converters. The half-bridge converter can be termed symmetric or asymmetric depending on how identical their switch driving signals are designed [17]. The advantage of bidirectional functionality is added in these proposed converters.

### 2.3. Bidirectional multiport converter

Isolated multiport converters with bidirectional functionality have been proposed and investigated. The classification as multiport implies that all sources can equally function as a load. The authors in Ref. [18], developed a group of bidirectional multiport converters by combining the magnetic coupling and DC-link functionalities. These converters boast of being low cost and simple. Another topology proposed [19] consisted of three half-bridges coupled by a transformer having high frequency and matching windings.

The energy transfer is attained through inductors $L_1$, $L_2$ and $L_3$. The inclusion of the boost HB implies that low input voltage sources can be used. The current-fed HB structure in port 3 of this converter is dissimilar to the voltage fed HB structure of the previous topology [18]. This connote that low current ripple can be accomplished in port 3 as the capacitor currents are reduced. The presence of soft switching is an advantage as the converter operated at high frequency thereby reducing switching losses.

The output voltage is given as:

$$V_0 = \frac{n_3}{n_1}V_1 + \frac{n_2}{n_1}V_2 \tag{3}$$

Similar works are proposed in Ref. [20] with the authors implementing soft switching by use of snubber capacitors and transformer leakage inductance. In Ref. [21], emphasis is placed on the converter application for lamp ballasts. The half-bridge configuration has been modified to consist of three full bridges in Ref. [22].

Jakka et al. [23], investigated the extension of the dual-active bridge to an asymmetrical triple active bridge. A three-leg converter is added on the secondary side with full bridges attached to separate transformer windings on the primary side. An advantage of this structure is the absence of direct leakage impedance and consequently, less leakage power. Direct leakage impedance is the combination of the resistance and leakage reactance, that exist in the primary and secondary windings of the transformer. The drawbacks are a high number of semiconductor switches and complex control.

The challenge associated with dual active bridge multi-port converters to achieve soft switching within wide power ranges is investigated in Ref. [24]. This topology introduces the application of a three-port inductor-inductor-capacitor (LLC) resonant converter. In this converter, each port has H-bridges with a resonant tank. The resonant tank consists of series resonant capacitor and inductor.

In [25], the three port converter has bidirectional capability, and employed a series resonant configuration. Half-bridge configuration is used with a split DC bus for switching to minimise the number of switches. ZVS and ZCS conditions are achieved by means of an LLC resonant tank configured on each port. The topology is illustrated in Fig. 3.

There are two modes of operation in each half-cycle. In mode 1, switches, $S_1$ & $S_2$ on the transformer primary side are turned on while switches $S_3$–$S_6$ on the secondary side are turned off. The freewheeling diodes of switches, $S_3$–$S_6$ stay on to ensure rectification. Under this condition, power is delivered from port 1 to ports 2 and 3. In the second operation mode, the switching sequence is reversed as switches $S_1$, and $S_2$ on port one are turned off, and switches, $S_3$, $S_4$, $S_5$ and $S_6$ are turned on. As in the first operation mode, there is rectification by the freewheeling diodes on port 1 thus ensuring that power transfer occurs from port two and port three to port one. This topology has the advantage of simple control as switching at every instant involves only ports providing power.

In [26], analysis was conducted on the power sharing operation. The model and rules have been established. In Ref. [27], the solid state transformer in the converter was modelled.

Additional buck-boost stages to port one and port three have been implemented in Ref. [28], by adding more switching cells. In Ref. [29], the converter has been designed for medium voltage DC grids.

In [30], the multi-element resonant tanks are configured in a series-parallel mode. In this converter, *Cr* and *Lr* are connected in series to a parallel pair of *Cp* and *Lp*. The converter achieved high efficiency. The drawback is the leakage inductor which causes adverse losses. In Ref. [31], the converter power coupling analyses was conducted.

### 2.4. Double input full-bridge boost converter with multi-winding transformer

In [32], the converter is a double input structure. Each input port has a current source formed by a boost inductor, prior to a full-bridge inverter. There are four transformer windings. They have equal turns number and ratio on the primary side. Another four-winding transformer is sandwiched between two full-bridge rectifiers at the secondary part. The converter operation is in three modes. In the first operation mode, every switch in the input port is turned on. Boost inductors, $L_1$ and $L_2$ are energized by the input sources. The diodes on the secondary are turned off, and the output capacitors serve the load. In the second mode, when switches $S_1$ and $S_4$ in input port 1, are turned on, the alternate pair of switches, $S_2$ and $S_3$, are turned off. The inductor, $L_1$ connects to the transformer windings through the conducting switches and diodes, $D_1$, $D_4$, $D_5$, $D_8$ conduct to serve the load. The third mode is same as the second mode except that components related to input port two are involved. In the second and third operating modes, simultaneous power delivery to the load is not feasible. In Ref. [33], the authors

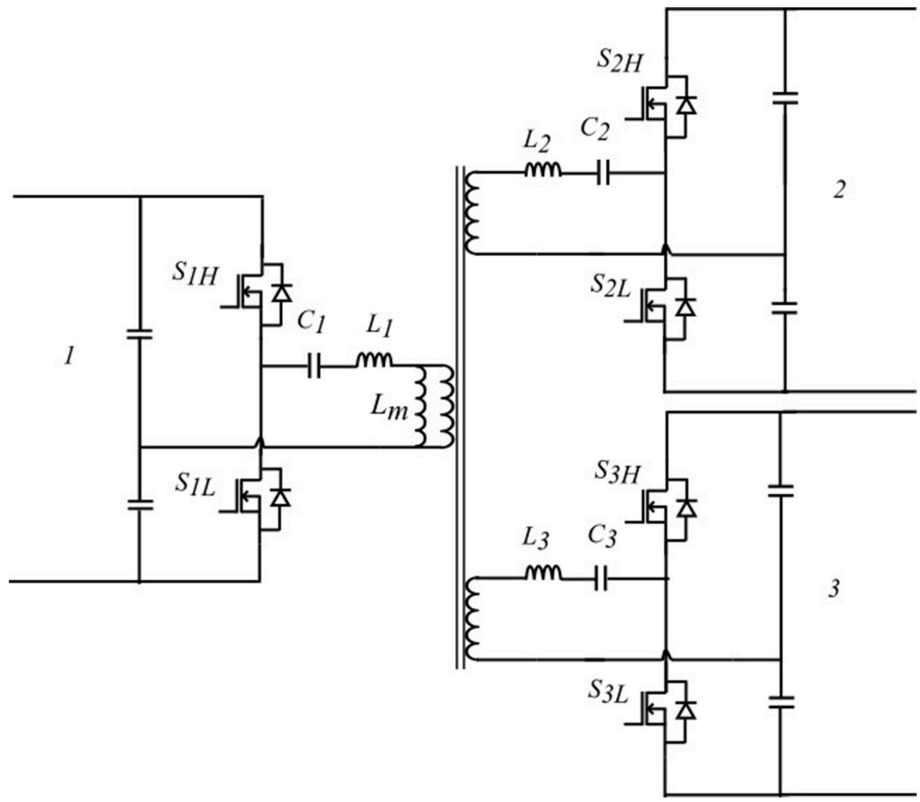


**Fig. 3.** Multiport resonant DC-DC converter [25].

performed more detailed analysis of the converter regarding common mode current attenuation, ground loop, magnetic integration and the mechanism for adding input sources.

The output voltage equation for the respective input voltages is given as:

$$V_o = V_1 \frac{n}{2(1 - D_1)} \tag{4}$$

$$V_o = V_2 \frac{n}{2(1 - D_2)} \tag{5}$$

In (4) and (5), $n$ represents the transformer turns ratio, $D_1$ is the duty ratio of switches in input port one and $D_2$ is the duty ratio of switches in input port 2. Equations (4) and (5) also show that the there is no relationship between $V_1$ and $V_2$ because input sources can only deliver power alternately.

Other shortcomings of this converter include lower efficiency due to the large number of semiconductors and complexity of transformer design.

Table 1 shows a summary of the properties of magnetically connected multi-input converters that have been reviewed.

## 3. Electromagnetically connected multi-input converters

### 3.1. Direct charge double input converter

Several authors have investigated electromagnetic multi-input converters. The topology proposed in Ref. [34] can be termed as a direct charge converter due to the presence of the battery storage port on the

**Table 1**
Summary of magnetically connected multi-input converters.

| Converter | Output Voltage | S | D | L | C | Drawbacks |
|---|---|---|---|---|---|---|
| Multi-input converter with buck-boost configuration [6] | $V_{out} = \frac{D_1}{N_1(1-D_1-D_2)}V_1 + \frac{D_2}{N_2(1-D_1-D_2)}V_2$ | 2 | 3 | – | 1 | Simultaneous power delivery lacking |
| Double input full-bridge converter [10] | $V_O = \frac{N_3}{N_1}V_1 + \frac{N_2}{N_1}V_2$ | 8 | 12 | 2 | 1 | Complexity of control |
| Bidirectional multiport converter [18] | $V_0 = \frac{n_3}{n_1}V_1 + \frac{n_2}{n_1}V_2$ | 6 | – | 2 | 7 | No control for battery charging |
| Bidirectional dual active transformer-based [23] | $V_o = \frac{NR_l}{2f_s}\left[\frac{V_1 D_{13}(1-D_{13})}{L_{f1}} + \frac{V_2 D_{23}(1-D_{23})}{L_{f2}}\right]$ | 14 | 14 | 2 | 1 | Large number of semiconductors |
| Bidirectional LLC resonant converter [24] | – | 12 | 12 | 3 | 6 | Large number of switches and diodes |
| Multiport resonant converter [25] | – | 6 | 6 | 3 | 9 | Power sharing challenges |
| Three port bidirectional converter [22] | – | 12 | 12 | – | 1 | Large number of switches and diodes |
| Full bridge with multi-winding transformer [33] | $V_o = V_1\frac{n}{2(1-D_1)}$<br>$V_o = V_2\frac{n}{2(1-D_2)}$ | 8 | 8 | 2 | 2 | Low efficiency, high parts count |
| S = switch, D = diode, L = inductor, C = capacitor<br>$R_L$ = Resistance | $N_1 = n_1$ = Number of turns for port 1<br>$N_2 = n_2$ = Number of turns for port 2<br>$N_3 = n_3$ = Number of turns for secondary winding<br>$D_{23}$ = Duty ratio of switches, S2 & S3<br>$L_{f2}$ = Equivalent inductance | | $D_1$ = Duty ratio of switch, $S_1$<br>$D_2$ = Duty ratio of switch, $S_2$<br>$D_{13}$ = Duty ratio of switches, $S_1$ & $S_3$ | | | |

DC link. There are respective half bridges on both the primary and secondary windings. The converter can operate in double input and double output mode. In the double output mode, the PV input charges the battery while delivering power to the load. The converter has three modes of operation. Initially, switches $S_3$ and $S_4$ are conducting whereas $S_1$ and $S_2$ are non-conducting. In the first mode, $S_3$ remains on, and $S_1$ turns on. $S_2$ remains off, and $S_4$ turns off. There is a positive voltage across the transformer. Second, $S_2$, $S_4$ are turned on and $S_1$, $S_3$ are turned off. The transformer has negative voltage applied. Third, $S_3$, $S_4$ are on, $S_1$, $S_2$ are off. There is zero voltage across the transformer. The output voltage is related to the input voltages as given:

$$V_2 = V_1 \frac{d_1}{d_1 + d_2} \tag{6}$$

$$V_o = 2nd_1 V_2 \tag{7}$$

In (6) and (7), $n$ is the transformer ratio, $d_1$ represents the duty ratio of switches $S_1$ and $S_4$, $d_2$ represents the duty ratio of $S_2$ and $S_3$. $V_O$ is the output voltage, $V_1$, $V_2$ are the input voltages.

This converter has an advantage of a low number of switches. $V_2$ can be charged if replaced with a battery. It is impossible to charge source, $V_1$ as a battery due to the presence of the diode. In Ref. [35], the converter is further extended to a family of converters that exhibit primary freewheeling, post regulation and synchronous regulation individually.

### 3.2. DC link with magnetically coupled converter

The DC-link with magnetic-coupling combination approach is further applied in Ref. [36]. While [18] presented and discussed the general principles for developing this family of converters, the converter in Ref. [36], investigated a topology applicable for FC and supercapacitor inputs. There are three HBs; two on the primary side (HB1 & HB2) and the third on the secondary side (HB3). HB2 and HB3 are configured to form a boost dual half-bridge. HB1 is bidirectional and connects the supercapacitor. There is an advantage of a smaller number of switches. The drawback is absence of soft switching in $S_1$ and $S_2$. Modifications in Ref. [37] proposed a mid-tapped transformer and expunged the capacitors $C_1$ and $C_2$.

The secondary side half-bridge in Ref. [35] was moved to the primary side in Ref. [38] to derive a boost-integrated full-bridge converter. Due to potential short circuit of battery, only alternate turn-on sequence is permitted for switches on the same leg. All switches have the same duty cycle. In Ref. [39], the authors investigated the ZVS properties of the combined boost and phase shift controlled full bridge converter.

In [40], voltage multiplier (VM) cells are combined with interleaved inductors on each power port on the primary, as shown in Fig. 4. The secondary side used diode rectifier. Although high voltage conversion ratio is present, the large number of switches is a disadvantage.

### 3.3. Tri-modal half-bridge converter

The converter proposed in Ref. [41] can be classified as tri-modal half-bridge converters. There is a half-bridge source and an active-clamp forward source. There are three switches $S_1$, $S_2$ and $S_3$. The topology is obtained by the inclusion of a free-wheeling diode and switch branch across the transformer. The switches have different duty cycles. The mode of operation is as follows. $S_1$, $S_2$ and $S_3$ are turned on in mode one, mode two and mode three respectively. During mode 1, the primary side of the transformer receives a positive voltage. In mode 2, the voltage is reversed, and charge or discharge operation of secondary source can happen. In mode 3, the transformer receives zero voltage. This topology has advantages of soft-switching, marginally reduced switch stress, and battery charging possibility. The drawback is that control of the battery charge and discharge functionality is not present.

Modifications in Ref. [42] replaced the connection point of capacitor $C_1$ from the battery terminal to ground. This gives greater control of battery charge or discharge. The authors focused on the control, voltage and current regulation of the input, output and battery. In Ref. [43], the converter has been extended to include solar, wind turbine, and battery inputs respectively.

### 3.4. Multiport converter with simultaneous power management

The converter introduced in Ref. [44] is able to boost the input voltages and incorporate MPPT converter capabilities. The converter, as illustrated in Fig. 5 assimilates different RE sources like wind turbines, solar cells, and fuel cells. The converter has three operation modes along with boost converter capability. In operation mode one, the transformer primary winding adopts the voltage of $C_1$ due to the turning-on of all switches and subsequent charging of all source inductors. Power transfer from one source to the output occurs in operation mode two when a

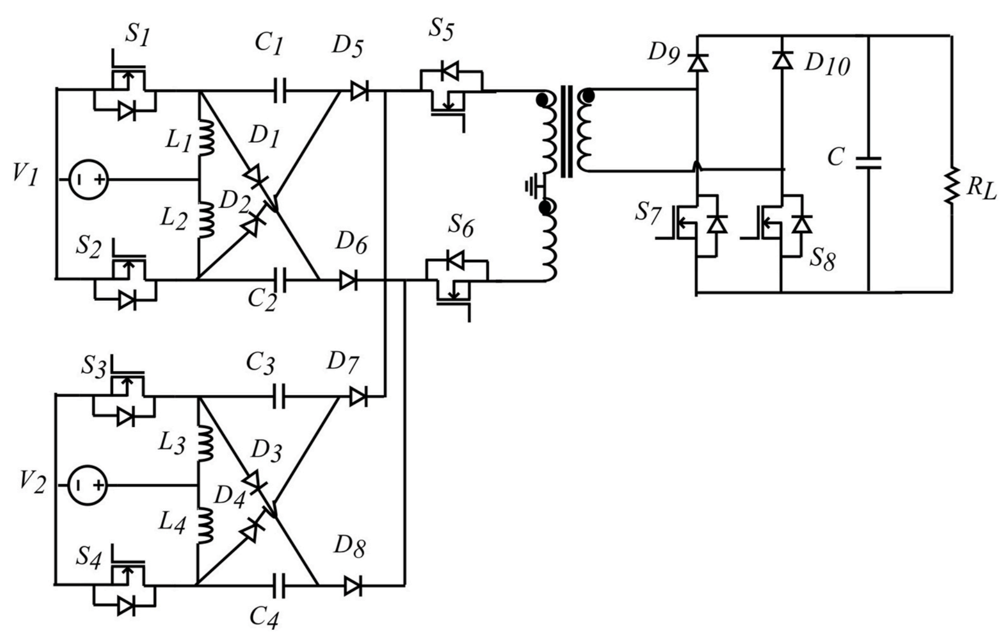


**Fig. 4.** Electromagnetic high gain converter [40].

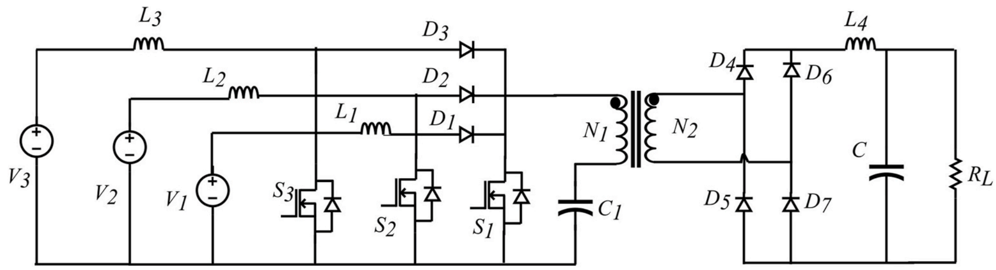


**Fig. 5.** Multiport converter with simultaneous power management [44].

single switch is turned on with all others turned off. In operation mode 3, all sources can transfer power to the output when all switches are turned off.

### 3.5. Three-level multi-input converter

In [45], pulsating current-source cells (PCSC) are inserted at the respective inputs and integrated in a three-stage structure on the primary side of the transformer. At the transformer secondary, the full bridge converter suffices. A half-bridge may be used in the secondary side also. The switching sequence is such that, $S_2$ is turned off after $S_3$ is turned on. After that, $S_4$ is turned on, and $S_1$ is turned off. When $S_1$ and $S_2$ are turned on, the boost inductors, $L_1$ and $L_2$ begin charging and the output capacitor, $C_o$ feeds the load. When $S_1$ and $S_2$ are turned off, the inductor delivers stored energy to the load.

While the converter has control over the output power of the input sources, in addition to existence of isolation between input and output ports, there is no control over battery charging.

### 3.6. Multiport boost converter with isolated and non-isolated ports

A converter that incorporated isolated DC port and non-isolated DC port was proposed in Ref. [46]. This was done by combining a modified half-bridge from Ref. [41] with a boost topology. The structure is depicted in Fig. 6. There are six operation intervals for this converter. In the first interval, $M_1$ is turned on, $D_3$ is forward biased and inductor $L_1$ charges. The input supplies the load. In interval 2, $M_1$ is turned off, the body diode of $M_2$ enables freewheeling of primary current. $D_3$ conducts and $L_1$ continues charging. PV unit and output capacitor deliver power to the load. In interval 3, freewheeling of primary current stops. $D_3$ is reverse biased. The capacitor, $C_{bus}$ serves the load. At interval 4, $M_2$ is turned on. $D_1$, $D_2$ are forward biased. The battery is charged from $C_2$ and PV input. $L_1$ and $C_3$ discharge to $C_1$, $C_2$. Output capacitor, $C_{bus}$ serves the load. For interval 5, $M_2$ turns off, body diode of $M_1$ allow freewheeling of primary current, $L_1$ discharges. Battery, $C_1$, $C_2$ are charged by PV input. Load is served by $C_{bus}$. In interval 6, $D_1$, $D_2$ are reverse biased after current freewheeling ends. $C_{bus}$ serves the load. This topology has advantages of ZCS operation on switches, and continuous input current.

The converter in Ref. [47] had three parallel legs to add an AC output port to the existing isolated and non-isolated ports. This converter has three switching states. In switching state A, when switches $S_1$ and $S_2$ are turned on and $S_3$ is turned off, capacitors $C_1$ and $C_2$ are charged. Inductor $L_1$ discharges. In switching state B, $S_1$ and $S_3$ conduct, and $S_2$ is turned off. The inductor continues discharging. $C_3$ charges whereas $C_1$ discharges. In switching state C, $S_2$ and $S_3$ are turned on, $S_1$ is turned off. $L_1$ and $C_1$ charge while $C_2$ is discharged.

### 3.7. Multiport converter with ZCS

Nareshkumar et al. [48], proposed a converter that is current fed and attains ZCS by use of a resonant tank formed by the high-frequency transformer leakage inductance with a parallel resonant capacitor. There are five operating modes. First, $S_2$ is turned on in addition to already conducting $S_1$. $D_1$, $D_2$ are on, $D_3$, $D_4$ are off. Energy in $L_{lk}$ is delivered to load. Second, status of switches remains the same but $S_1$ current declines whereas $S_2$ current appreciates towards resonance. Third, $S_1$ achieves ZCS as its body diode allows reverse current conduction. Fourth, $D_3$, $D_4$ turn on with $S_2$ already on. Resonant capacitor, $C_p$, charges from inductor $L_1$. Fifth, conducting elements are $S_2$, $D_3$, $D_4$. $V_1$ delivers energy to the load.

Further modification by the same authors [49], included a series resonant capacitor and a 5-level inverter. The positive attribute of this converter is the low switch count. The downside is the complexity of control due to a combination of frequency modulation and duty ratio variations.

Lin et al., [50], excluded the resonant tanks. However, the topology is extended to accommodate a four-port converter. The topology had two PCSC input sources followed by full-bridge configurations on the

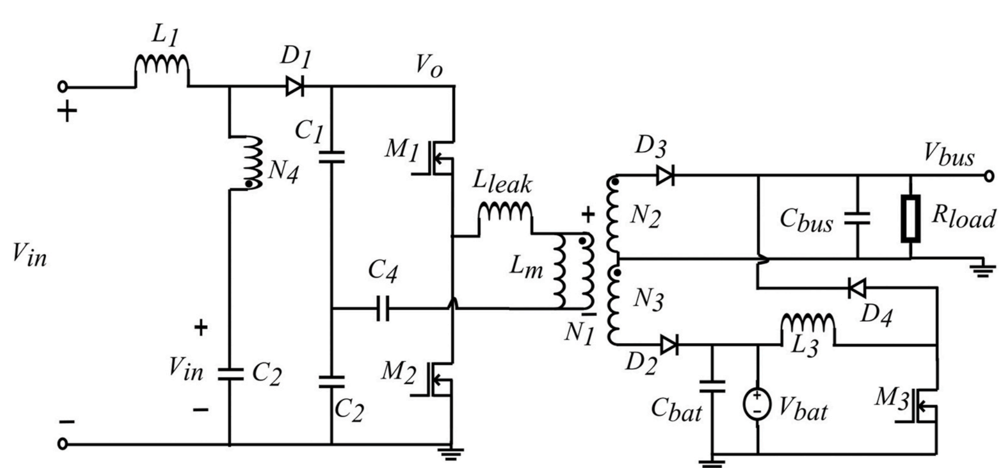


**Fig. 6.** Multiport boost converter with isolated and non-isolated ports [46].

respective low voltage winding and high voltage windings of the transformer. There is a large voltage transfer ratio (VTR) and soft switching.

The advantage of a wide input voltage range is highlighted in Ref. [51]. The authors proposed a full-bridge three port converter. The absence of soft switching is a major drawback of this topology.

### 3.8. Bidirectional converter with multiple combined battery storage input sources

Karthikeyan & Gupta [52], investigated a combination of series connected battery storage as multiple inputs. The converter is bidirectional. The series battery storage is followed by a bridge stage on both windings of the transformer. For a three-input converter, the switching for charging and discharge of the battery storage inputs are further explained. The converter can operate in single input mode or combined input mode. For battery input 1 to operate in single input mode, $S_1$, $S_5$ and $S_6$ are turned on. Battery charging occurs when $S_5$, $S_6$ are turned on, and $D_1$ is forward biased. When $D_5$, $D_6$ are forward biased, and $S_1$ is turned on, the battery is discharged to the load. In the combined input state, the switching sequence causes the series connection of the inputs, thereby doubling the voltage in the primary side and resulting in higher transfer of power to the load. In order to operate a battery input in combination with another, the switch and anti-parallel diode in series with the desired battery input is turned on. To deliver power from all three sources, $V_1$, $V_2$, $V_3$, switches $S_1$, $S_2$, $S_3$ and diodes $D_1$, $D_2$, $D_3$ are turned on. When $S_4$ and $D_4$ are turned off, $V_1$ is excluded from the battery combination. Thus, turning off the parallel switch and diode connected to each input source will prevent it from receiving or delivering power. The modification of the dual active bridge configuration attained reduced circulation power, peak stress and improved efficiency. The drawback is the increased semiconductor count as number of battery inputs increase. Sophisticated control is also a weakness.

Table 2 shows a summary of the properties of electromagnetically connected multi-input converters that have been examined.

**Table 2**
Summary of electromagnetically connected converters.

| Converter | Output Voltage | S | D | L | C | Drawbacks |
|---|---|---|---|---|---|---|
| Direct charge double input converter [34] | $V_o = n[D_1(V_1 - V_2) + D_2V_2 = 2nD_1V_2$ | 4 | – | 2 | 3 | Uncontrolled battery charge and discharge |
| Combined DC link and transformer [36] | $V_{load} = nV_{dc}$ | 6 | – | 2 | 5 | No soft switching |
| Boost-integrated full-bridge converter with phase-shift for three port interface [38] | $V_0 = 2.\Phi_{eff}.n.V_1$ | 4 | 4 | 2 | 3 | Voltage limit |
| Tri-modal bridge converter [41] | $V_o = \frac{2d_1d_2}{d_1+d_2}nV_1$ | 3 | 3 | 1 | 3 | Uncontrolled battery charge and discharge |
| Converter with wide input voltage range using full bridge [51] | $V_o = 2nd_3V_2$ | 4 | 4 | 1 | 1 | No soft switching |
| Multiport simultaneous power management converter [44] | – | 3 | 7 | 4 | 2 | High number of magnetic elements |
| Multi-input three-level converter [45] | – | 4 | 8 | 3 | 3 | Uncontrolled battery charge and discharge |
| Three-port converter for PV-battery [46] | $V_o = V_1 + \frac{N_4}{N_3}V_2$ | 3 | 4 | 3 | 6 | |
| Converter with DC and AC output [47] | $V_{dcout} = V_{dcin}\frac{1}{1-d}$ $V_{an} = V_{dcin}\frac{m_{ai}.d}{\sqrt{3}(1-d)}$ | 9 | 5 | 1 | 2 | Complex control |
| ZCS boost converter [48] | – | 2 | 4 | 3 | 2 | Complex control, modulation challenges |
| Four-port bidirectional full-bridge converter [50] | – | 10 | 12 | 3 | 3 | High parts count |
| High gain multi-input converter [40] | – | 8 | 18 | 1 | 1 | High switch and diode count |
| Bidirectional converter with multiple combinational battery storage inputs [52] | $V_{out} = \sum_{i=1}^{m} V_{in}$ | 14 | 14 | 1 | 1 | Sophisticated control, high switch and diode count |

S = switch, D = diode, L = inductor, C = capacitor

## 4. Electrically connected multi-input converters

### 4.1. Synthesis of electrically connected multiple input DC-DC converters

Kwansinski [53], examined the possibility of transforming several traditional single input converters to multiple input converters. This was done by establishing four rules that could assist the designer in the realisation of the desired converter. Following these rules stringently, only buck and buck-boost converters can be transformed. Extension of other converter types becomes possible when the rules are modified. For example, the Cuk and single-ended primary inductance converter (SEPIC) were realized by applying time-multiplexing control.

Liu & Chen [54], introduced a construct for the pulsating voltage-source cell (PVSC) and the PCSC. Generally referred to as pulsating source cells (PSC), their addition to the basic PWM converters resulted in multiport converters. The converters had source utility; hence the different sources can serve the load both singularly and collectively. More illumination on the use of PSCs in synthesising multi-input converters was provided in Ref. [55].

Li et al. [56], identified PSCs and an output filter cell (OFC) as the basic components of multi-input converters. Also, different types of OFCs, PVSC, and PCSCs were identified. Different combinations of the identified PSCs and OFCs produce two variants of multi-input converters from the basic non-isolated PWM converters. The concept was extended to magnetically connected and electromagnetically connected multi-input converters. Chen et al. [57] restricted their investigation to integrating single-input double-output and double-input single-output models for the basic converters.

### 4.2. DC-DC converters in series or parallel

Series or parallel connection of converters was the first attempt at developing multiple inputs in non-isolated converters. The foremost topology was introduced by Solero et al., [58], where the electrical series connection of two boost converters is used for battery charging. The topology is illustrated in Fig. 7. This converter makes use of solar array and wind generator as the input sources. The output voltage, $V_o$ is given as:

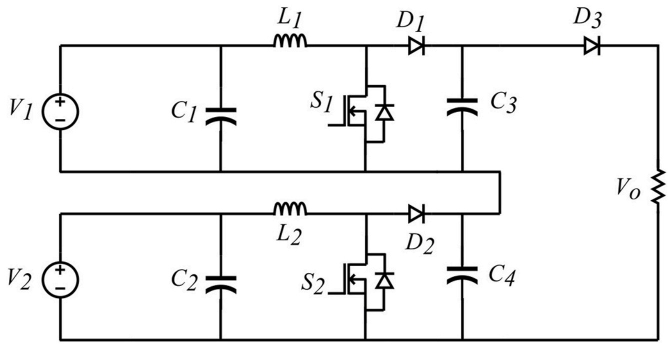


**Fig. 7.** Series connected DC-DC converters [58].

$$V_o = \frac{V_1}{1 - D_1} + \frac{V_2}{1 - D_2} \tag{8}$$

$V_1$ and $V_2$ are the respective input voltages, $D_1$ is the duty cycle of switch $S_1$, and $D_2$ is the duty cycle of switch $S_2$.

Two parallel coupled buck converters are introduced in Imes & Rodriguez [59]. Further work in Ref. [60] examined the stability and dynamic behaviour of the converter. The parallel bidirectional coupling of three converters is proposed in Ref. [61]. Each module has two switches and an inductor with buck and boost configuration. If conditions require power transfer to the load, the boost function is implemented by switch $Q_2$ and diode $D_1$. Battery charging occurs with the buck function by the operation of switch $Q_1$ and diode $D_2$. This topology is advantageous for the ease of harnessing differing voltage sources unlike in Refs. [59,60]. The shortcoming is the absence of soft switching.

The output voltage is given by:

$$V_o = \frac{V_1}{1 - D_2} = \frac{V_2}{1 - D_4} = \frac{V_3}{1 - D_6} \tag{9}$$

$V_1$, $V_2$ and $V_3$ are the input voltages, while $D_2$, $D_4$ and $D_6$ are the duty cycles of switches $Q_2$, $Q_4$, and $Q_6$ respectively.

The modified converter investigated in Ref. [62], created specific buck or boost operation modes for each FC, ultracapacitor (UC) and battery unit. The converter also used a common output filter, thus the number of capacitors reduced. The topology is presented in Fig. 8.

The multiport bidirectional converter in Ref. [63] also used a parallel connection of buck/boost cells but eliminated the DC-link capacitor thereby increasing efficiency. Control of the topology as applicable to interfacing multiple microgrids is examined in Ref. [64].

More series or parallel connections of diverse converter configurations are investigated in Ref. [65]. The parallel connection of a buck/-boost converter and a forward converter in Ref. [66] yielded a double input converter for battery charging.

Other authors have investigated different topologies in series or parallel. The switched diode-capacitor converter in Ref. [67] targeted voltage summation. In Ref. [68], The converter performance was investigated. Summation of the input voltages achieved high step-up capacity.

### 4.3. Double input DC-DC converter

Traditional buck-boost and buck converters were modified to include two voltage sources in Ref. [69]. The topology is presented in Fig. 9. There are high voltage and low voltage input sources denoted by $V_H$ and $V_L$, respectively. The output voltage, $V_o$ can neither be more than $V_H$ nor less than $V_L$. This challenge was solved in Ref. [70] by including the inductor in the PVSC structure. During turn-on state for either of switches $S_H$, $S_L$ or both, power transfer from the source (s) to the output takes place. At turn of state, the diodes $D_H$ and $D_L$ complete the circuit thereby releasing energy stored by the inductor.

The output voltage is defined by;

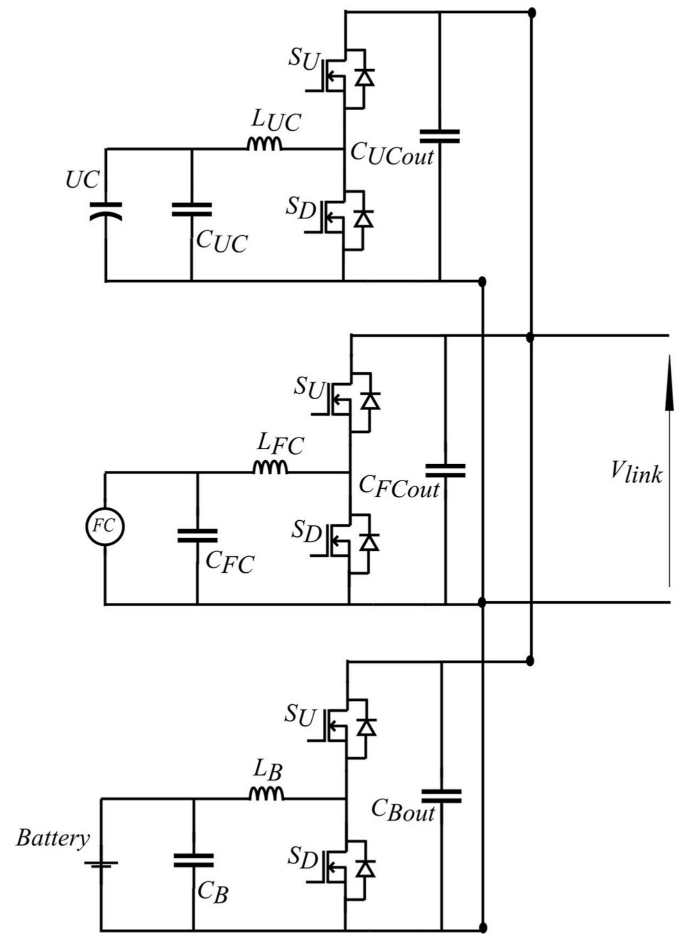


**Fig. 8.** Parallel connected converters [62].

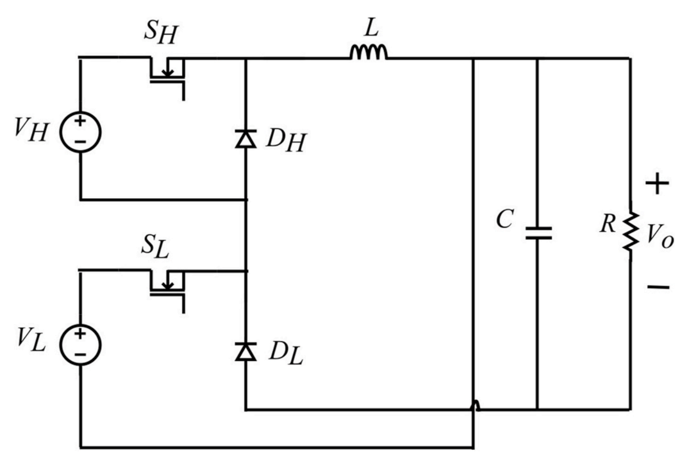


**Fig. 9.** Double input DC-DC converter [69].

$$V_O = \frac{d_H}{1 - d_L} V_H + \frac{d_L}{1 - d_L} V_L \tag{10}$$

where $V_O$ is the output voltage, $V_H$ is the high voltage input, $V_L$ is the low voltage input, $d_H$ is the duty ratio of the high voltage switch, $S_H$ and $d_L$ is the duty ratio of the low voltage switch, $S_L$.

The presence of soft switching and the ability to harness different voltage levels without the use of transformers suffice as advantages of the converter. Absence of battery charging, and maximum output voltage limited to $V_H$ are drawbacks.

Kanhav & Chaudhari [71], added the bidirectional feature by replacing the upper diode with a third switch. The converter also lacks battery charging feature.

In [72], the authors introduced two-input integrated buck-buck converter. The buck-buck converter applied two PVSC cells for the input sources. Looping the ground to the inductor output achieved a buck-buckboost converter.

In [73], Gummi et al. investigated using a single-pole-triple-throw (SPTT) switch to develop double input converters. Another investigation to use H-bridges to build the double input converter has been done in Ref. [74].

A double input buck-boost/buck-boost converter was proposed in Ref. [75]. Here, the output voltage depends on the charging time of the inductor. Battery charging is made possible in this structure.

The converter in Ref. [76], is a buck-boost/buck topology. It was applied in electric vehicles' storage systems.

In [77], the coupled inductor topology is applied for improvement of the FC and UC dynamic response. The converter is bidirectional.

In [78], the sources can feed the output only, or serve the load while charging a selected input in either mode. An additional input source can be created by attaching an inductor-switch-diode branch to the existing inductor. This converter is suitable for a PV-battery system.

Sun et al. [79], proposed a bootstrap circuit formed by charging switch and a series connection of double input buck/buck converter. Fault tolerance when short-circuit of one input occurs is an added advantage.

In [80], simultaneous power transfer is made possible by two power switches. The structure accepts a wide input voltage range. Individual power delivery depends on an auxiliary diode. The need for a threshold voltage before the secondary input source can transfer power to the load is a weakness of this structure.

In [81], a similar double input buck/buck converter is introduced. The soft switching is achieved using inductive and capacitive circuits interfaced with the respective input ports. In Ref. [82], the position of the inductor and capacitor branches have been interchanged. The authors examined the performance of the converter in boundary conduction mode [83]. By combination of the hybrid inductor and capacitor buck cells, a dual buck inductor-capacitor (LC) converter was developed in Ref. [84]. The performance of the LC buck converter with PV and wind turbine as input sources in a standalone generation system have been investigated in Ref. [85]. Further, in Ref. [86], the LC converter has been integrated with a grid system.

In [87], the double input converter is a parallel connection of a buck converter and a SEPIC converter. This integration has the benefit of decreased component count. Further steady-state analyses of the converter have been conducted in Ref. [88].

In [89], secondary battery storage is connected in parallel to the voltage inputs. The power switches are operated in a way that the battery can be charged by the input voltage when necessary and deliver power to the load through a traditional boost converter. The converter has low number of components.

Additional double input structures for a mixture of the traditional converters were introduced. In Ref. [90], a buck/buck converter having a soft-switching feature was introduced. Similarly, there is a SEPIC/SEPIC structure in Ref. [91]. The converter is a double input SEPIC converter. A control strategy based on decentralised controller is proposed in Ref. [92]. In Ref. [93], isolation between input ports and the output was achieved.

In [94], battery "charge and discharge" function was added to the multiple input sources of the SEPIC converter.

In [95], the multiple input Cuk structure is equipped with edge-resonant soft switching. This improved the efficiency of the converter. Another multi-input Cuk converter in Ref. [96], had a resonant switch with resonant components at the respective inputs. The authors identified and applied principles to synthesise double input Cuk/SEPIC structure in Ref. [54]. The converter in Ref. [97], has a high step-up using boost structure.

### 4.4. Multi-input buck-boost converter

In [98], the input sources are connected in parallel after their respective power control switches. A conventional buck-boost configuration is used. Hence the operation is similar except for the control of the input voltages. Minimal components and simple control are advantages. Some weaknesses are the inability of simultaneous power transfer by the input sources, negative reference output voltage and absence of bidirectional operation. The negative output voltage can be reversed using a transformer.

Khaligh et al. [99], introduced two additional switches to the topology. These switches take care of bidirectional operation and the negative output voltage. The circuit is shown in Fig. 10. It can operate as buck, boost and buck-boost. Although all sources can deliver power in the buck mode, the problem persists in the boost mode of operation.

For a buck mode operating two-input converter, output voltage is given as:

$$V_{out} = D_1 V_1 + (D_2 - D_1) V_2 \tag{11}$$

In (11), $D_1$ is the duty ratio of $Q_1$, $V_1$ is the voltage of the first input source, $D_2$ is the duty ratio of $Q_2$ and $V_2$ is the voltage of the second input source.

### 4.5. Multi-input DC-DC converter based on switched-capacitor/diode capacitor/switched inductor

Cheng & Yuan-mao [100], eliminated the use of magnetic elements in the design of two input converter based on switched capacitors (SC). The structure has three switches operating at 50% duty cycle. There are four operating modes. The two main power switches, $S_1$ and $S_2$ are turned on at the same time. In the first mode, at the turn-on of $S_3$, $S_1$ and $S_2$ remain turned off. $V_2$ charges $L_1$ and $C_1$, $V_3$ charges $L_2$ and $C_2$, while the circuit operates at resonant frequency. In the second operation mode, resonance operation is cut short as all switches are turned off. In the third operation mode, a series connection of $V_2$ with $L_1$, $C_1$, $L_2$ and $C_2$ is developed by turning on $S_3$, $S_2$ and diode, $D_3$. Thus, energy is transferred to the load by the discharging inductors and capacitors. During the fourth operation mode, diode $D_3$ is turned off while $S_1$ and $S_2$ remain turned on. The output capacitor supplies the load. The output voltage is the total of the respective input voltages.

$$V_{out} = V_1 + V_2 + V_3 \tag{12}$$

This converter is termed a multi-input voltage summation converter. The converter suffers from high output ripple and output leakage voltage.

The elements have been rearranged in Ref. [101] to achieve a multi-input voltage subtracting converter.

In [102], the SC cells are arranged in a multilevel structure. The circuit is shown in Fig. 11. The current fed input is used to keep input ripple low. The converter operates in two modes. In the first mode, the two inputs deliver power to the load. In the second mode, one input charges the second input. For the transfer of power to the load by the two inputs, the load is fed by capacitors, $C_1$, $C_3$, $C_5$ when switches, $S_1$ and $S_2$ are turned on, and $S_3$ is turned off. Energy from $V_1$ is delivered to the load and output capacitors when only $S_1$ is turned on.

The voltage gain for a three-level SC structure is given as:

$$\frac{V_o}{V_{1,2}} = \frac{3}{1 - D_{1,2} - D_3} \tag{13}$$

In (13), $V_o$ represents the output voltage, $V_{1,2}$ represents the average of the input voltages, $D_{1,2}$ are the duty ratios of switches, $S_1$ and $S_2$ and $D_3$ is the duty ratio of $S_3$.

An advantage of this converter is that the application of the SC cells

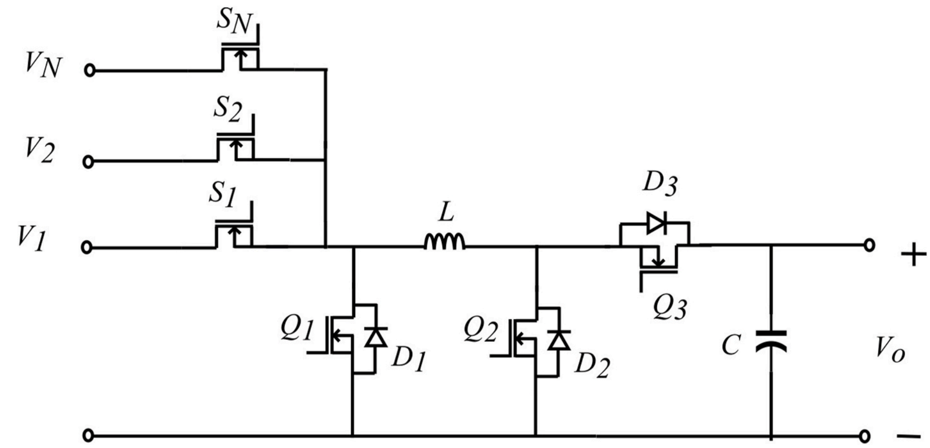


**Fig. 10.** Multi-input bidirectional buck-boost converter [99].

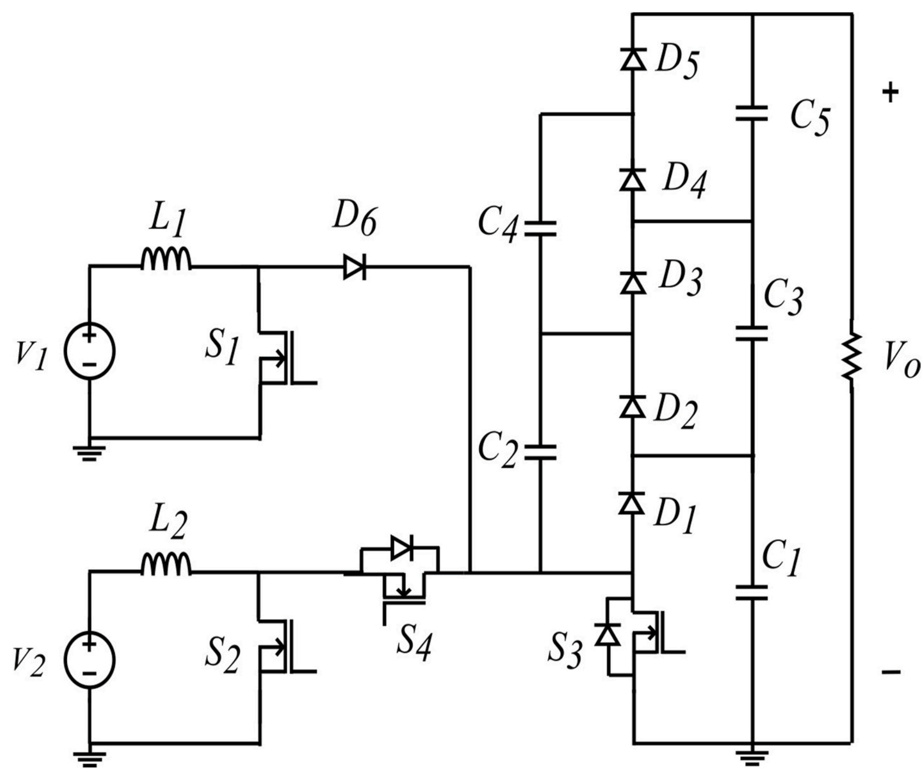


**Fig. 11.** Two input converter with three level switched-capacitor cells [102].

resulted in a high voltage gain for the converter. A drawback is the large number of passive elements.

A similar converter in Ref. [103], had lower voltage gain than [102] by making use of only one SC stage.

In [67], series and parallel connections of double input switched-diode capacitor converters in voltage accumulator mode were investigated. There is not much difference in structure and voltage gain when compared to the SC voltage summation converter. The converter has the advantage of low voltage stress and current stress for the components. In Ref. [68], series-parallel variations have been investigated.

Mahmoodieh & Deihimi [104], applied switched inductors to attain high voltage gain. The primary input is a battery storage that can be charged by other input sources when depleted. The converter can operate in three modes, like in Ref. [105]. In this converter, both the battery charge and discharge capability is not limited to duty ratios of the input sources. Hence, a unified system exists. The converter also has high efficiency. The drawback is large number of magnetic elements.

### 4.6. Buck/boost-boost based multi-input converter

Banaei et al. [106], proposed a combination of the buck/boost and boost topologies. The modularity of this converter implies that it is robust and can control the input sources independently. For this two-input model, the VTR is given as:

$$V_o = \frac{V_2}{1 - D_2} + \frac{D_1 D_2}{(1 - D_1)(1 - D_2)} V_1 \tag{14}$$

In (14) $V_o$ represents the output voltage, $V_1$ and $V_2$ are the input voltages, $D_1$, $D_2$ are the duty ratios of switches, $S_1$ and $S_2$.

The converter has advantages of low current stress and flexible control. The drawback is that as the number of input sources increases, the number of magnetic elements and switches increase just as the voltage and current ratings of the switches.

### 4.7. Three switches leg based multiple input converter

Azizi et al. [107], investigated current fed input attached to three switch inverter structure. The foremost leg is formed by $V_1$, $L_1$, $S_1$, $S_2$ and $S_3$. The number of inputs increase with additional legs and accompanying elements. The four uppermost switches in the structure form an inverter. In the boost operation mode, when $S_3$, the lowest switch on a leg is turned on, $L_1$ charges. When $S_3$ is turned off, the anti-parallel diodes of the middle and upper switches ($S_1$ & $S_2$) serve as the conduit for the capacitor to charge on the leg. The converter can output both AC and DC. The converter can function in the step-up mode and step-down mode. The advantage of low count for passive elements exists for this converter. The shortcomings are the absence of soft-switching and the modulation index limitation.

### 4.8. Multi-input converter with ZVS

In [108], the authors implemented ZVS for the switches by the use of an auxiliary circuit. Current source type inputs are operated in single input and dual input states. Table 3 shows the switch configurations and charging states for the operation time intervals. In the dual state, conduction losses are reduced. There is also high efficiency. However, the voltage stress of switches and diodes is high. In Ref. [109], the auxiliary circuit consist of two parallel diodes, inductor, an auxiliary switch and capacitor. The ZVS operation helped to achieve high efficiency.

In [110], an active clamp and quasi-resonant buck-boost configuration has been added to the existing structure. High voltage gain was achieved in addition to ZVS. However, the parts count remains high because of the auxiliary circuits.

### 4.9. Three-input boost converter for RE sources and energy storage applications

In [111], each of two input sources connected separately to a boost converter. $V_1$ and $V_2$ are PV cell and fuel cell respectively. The third source, $V_3$ is a battery attached to a full-bridge configuration. Switches $S_1$ and $S_3$ control power flow from input source $V_1$ just as switches $S_2$ and $S_4$ control that of source $V_2$. When the respective control switches are turned on, the input voltage charge the inductor. In turn off state, power from the voltage input is transferred to the load.

The battery input, $V_3$, is controlled by the following combination of switches. For charging purposes, switches, $S_2$ and $S_3$ are conducting but $S_1$ and $S_4$ are turned off. Battery discharging occurs when switches $S_1$ and $S_4$ are conducting. The output voltage is given as;

$$V_o = \frac{V_1 + d_4 V_3}{1 - d_1 - d_4} \quad (15)$$

$$V_o = \frac{V_2 + d_3 V_3}{1 - d_2 - d_3} \quad (16)$$

Equation (15) describes the output voltage for the combination of PV input source, $V_1$ and battery, $V_3$. Equation (16) describe output voltage for fuel cell input source, $V_2$ and battery, $V_3$. $V_o$ is the output voltage, $d_1$, $d_2$, $d_3$, $d_4$ are the duty ratios of $S_1$, $S_2$, $S_3$, $S_4$.

**Table 3**
Operation modes of multi-input ZVS converter [108].

| Interval | $S_1$ | $S_3$ | Operation |
|---|---|---|---|
| 1 | 1 | 0 | L1 charges, $iL_3$ is zero |
| 2 | 0 | 0 | C1 and C3 charging |
| 3 | 0 | 0 | D3 conducts |
| 4 | 0 | 1 | S3 in ZVS |
| 5 | 0 | 0 | S3 turned off, C1 and C3 charging |
| 6 | 0 | 0 | D1 conducts |
| 7 | 1 | 0 | S1 in ZVS |

Some drawbacks of this structure are that the load cannot charge the battery and there is arbitrary battery charge and discharge, which can reduce battery life.

In [112], the full-bridge converter was excluded and the battery input connected to charge or discharge in series with the PV cell source. This modification had two boost converters in use. A model and control strategy for three input PV/FC/battery converters was investigated in Ref. [113]. The converter functions in three modes. In the first mode, battery state of charge is optimal, and PV cell and fuel cell service the load. In the second mode, there is insufficient power from the PV and FC. Thus, the battery discharges to the load alongside the power sources. The third mode is when the power sources charge the battery and supply the load simultaneously. Power control of input sources, $V_1$ and $V_2$ is achieved by switches $S_1$ and $S_2$ respectively. The battery is charged by $V_1$ and $V_2$ with $S_1$, $S_2$ turned on and $S_3$, $S_4$ turned off. Battery discharge to load occurs when all switches are turned on. When $S_1$ and $S_2$ are turned off, $V_1$ and $V_2$ supply the load. The relationship between the input voltage and the output voltage for the different operation modes are:

Mode 1:

$$V_o = \frac{V_1}{1 - d_1 - d_4} = \frac{V_2}{1 - d_2 - d_4} \quad (17)$$

Mode 2:

$$V_o = \frac{V_1}{1 - d_1 - d_3} = \frac{V_2}{1 - d_2 - d_3} \quad (18)$$

Mode 3

$$V_o = \frac{V_1}{1 - d_1 - d_3} = \frac{V_2}{1 - d_2 - d_3} \quad (19)$$

In [114], a bidirectional load is served with the aid of a low frequency switch. This converter has the same voltage gain with the traditional boost converter.

In [115], three input ports have been added. The structure is similar to Ref. [116], albeit with only one output port.

Kardan et al. [105], used a boost configuration for the fuel cell, and buck/boost configuration for the PV cell and battery. Arbitrary battery charge and discharge is eliminated using four independent switch duty ratios in three different operation modes. The operation modes are the same as in Ref. [112]. The switch configuration for the respective modes is presented in Table 4.

The voltage gain of the converter is given by:

**Table 4**
Operation modes of new three input boost converter with high voltage gain [105].

| Mode 1: Battery bypassed, V1, V2 supply load | | | | | | | | |
|---|---|---|---|---|---|---|---|---|
| State | $S_1$ | $S_2$ | $S_3$ | $S_4$ | $L_1$ | $L_1$ | C | $C_o$ |
| 1 | 1 | 0 | 0 | 1 | C | D | C | D |
| 2 | 1 | 1 | 0 | 1 | D | C | D | D |
| 3 | 1 | 0 | 0 | 1 | C | D | C | D |
| 4 | 0 | 0 | 0 | 0 | D | D | C | C |
| **Mode 2: V1, V2 and battery supplying load** | | | | | | | | |
| **State** | **$S_1$** | **$S_2$** | **$S_3$** | **$S_4$** | **$L_1$** | **$L_1$** | **C** | **$C_o$** |
| 1 | 1 | 1 | 1 | 1 | C | C | D | D |
| 2 | 1 | 1 | 0 | 1 | D | C | D | D |
| 3 | 1 | 0 | 0 | 1 | C | D | C | D |
| 4 | 0 | 0 | 0 | 0 | D | D | C | C |
| **Mode 3: V1 and V2 supply battery and load** | | | | | | | | |
| **State** | **$S_1$** | **$S_2$** | **$S_3$** | **$S_4$** | **$L_1$** | **$L_1$** | **C** | **$C_o$** |
| 1 | 1 | 1 | 1 | 0 | C | C | D | D |
| 2 | 1 | 1 | 0 | 1 | D | D | D | D |
| 3 | 1 | 0 | 0 | 1 | D | D | C | D |
| 4 | 0 | 0 | 0 | 0 | D | D | C | C |
| Key- C: Charging D: Discharging | | | | | | | | |

$$\frac{V_o}{V_{1,2}} = \frac{1 + D^2 - D}{(1 - D)^2} \tag{20}$$

In (20), $V_o$ is the output voltage of the converter, $V_{1,2}$ is the summation of the input voltages at any instant, $D$is the duty ratio of the switches.

This configuration has a high step-up capability compared to conventional converters. The high number of passive elements and increased dissipation loss are drawbacks of this configuration.

### 4.10. Bridge type dual input converter

In [117], the bridge structure allows both input sources to supply power both singularly and collectively to the load. The converter is bidirectional. There are four switches. Switches, $S_1$, $S_2$, and $S_3$, determine the individual and simultaneous power delivery. Switch $S_4$ and diode $D_3$ control bidirectional operation. A combination of $S_4$, $D_1$ and $D_2$ influence buck, boost or buck-boost operation mode as necessary for the converter. There are four operation modes for the source to load power flow.

Mode 1:

Switch S1 is turned on. All other switches and diodes do not conduct. The single input voltage, VS1 charges the inductor. The load is supplied by the capacitor, C.

Mode 2:

The dual input function is exhibited in this mode. S3 is turned on. All other switches and diodes are turned off. VS1 and VS2 charge the inductor. Output capacitor continues to supply the load.

Mode 3:

S2 only is turned on. This is a single input operation. VS2 charges the inductor. The capacitor, C serves the load.

Mode 4:

Diode D4 conducts after S1, S2 and S3 are turned off. Neither VS1 nor VS2 can charge the inductor. Thus, the inductor discharges to the capacitor and the load.

For the load to source power flow, there are two additional modes.

Mode 5:

$S_4$ only is turned on. Load, $V_o$ charges the inductor. This is applicable in EVs regenerative braking.

Mode 6:

S4 is turned off. D3 conducts. Stored inductor energy flows towards VS1 and VS2.

Further performance analysis of the modified bridge type converter was conducted in Ref. [118] indicated efficient energy utilisation by the converter. This converter is unidirectional. Replacing the output diode with a bidirectional switch allow will permit reverse power flow. The output voltage of this converter is given as:

Buck mode;

$$V_o = V_1 d_1 + V_2 d_2 + (V_1 + V_2) d_3 \tag{21}$$

Buck-boost mode;

$$V_o = \frac{V_1 d_1 + V_2 d_2 + (V_1 + V_2) d_3}{(1 - d_1 - d_2 - d_3)} \tag{22}$$

Boost mode;

$$V_o = \frac{V_1 (d_1 + d_3) + V_2 (1 - d_1)}{(1 - d_1 - d_3)} \tag{23}$$

Some advantages of this family of converters are simple structure, easy control, bidirectional operation and low component count. However, the problems associated with traditional converters, like high input current and output voltage ripple, switch voltage stress, persist.

Table 5 shows the working modes, conducting elements and the direction of power flow for the boost unidirectional dual input bridge type converter [118]. In Ref. [119], three relay switches are positioned in other to achieve bidirectional operation.

**Table 5**
Boost operation modes of dual input bridge type converter [118].

| Mode | Sources supplying | Conducting elements | Power flow | L | C |
|---|---|---|---|---|---|
| 1 | $V_1$ | $S_1$, $S_m$ | Forward | Charging | Discharging |
| 2 | $V_1 + V_2$ | $S_3$, $S_m$ | Forward | Charging | Discharging |
| 3 | $V_2$ | $S_2$, $D_2$ | Forward | Discharging | Charging |

### 4.11. High VTR converter with voltage multiplier

In [120], the converter has a high VTR of 20. Two current fed inputs are followed by four stages of diode-capacitor VM cells. The switches control power transfer to the load by the voltage sources. The VM stages in addition to the continuous input current contribute to the high voltage gain. There are three operation modes in this converter. In the first operation mode, switches, $S_1$ and $S_2$ are turned on and sources, $V_1$ and $V_2$ charge the inductors. The output capacitor, $C_o$ supplies the load since the diodes in the VM stages are reverse biased. In the second operation mode, $S_1$ is turned off whereas $S_2$ is turned on. Since there is an even number of VM stages, diode $D_o$ is forward biased, and power flows from inductor, $L_1$ to the load. In the third operation mode, $S_1$ is turned on while $S_2$ is turned off. The output capacitor, $C_o$ supplies the load.

The output voltage is given as:

$$V_o = 3\frac{V_1}{(1 - d_1)} + 2\frac{V_2}{(1 - d_2)} \tag{24}$$

This converter has the advantage of high VTR and simple control. The design lacks bidirectional capability. There is high dissipation loss as a result of large number of passive elements. There is also lower efficiency as power requirements increase.

In [121], the number of inputs and VM stages are increased. This was further modified to a multi-input multi-output (MIMO) configuration in Ref. [122].

In [123], an auxiliary zero voltage transition (ZVT) circuit was added after the VM stages in order to reduce switching losses. The voltage stress on the diodes is less although there is a large number of diodes.

### 4.12. Modular high VTR multi-input converter

In [124], the additional input sources are stacked on the primary input source. The topology is shown in Fig. 12. The primary unit has a source, $V_1$, two switches, $S_0$ and $S_1$, two inductors, two capacitors and an output diode, $D_o$. Each additional input voltage source is complemented by an inductor, a switch, a capacitor and a diode. $S_0$ and $S_1$ have the same duty ratio. There are four modes. In mode 1, all the switches are turned on. All diodes do not conduct, and the inductors are charged. The output capacitor, $Co$ supplies the load. In mode 2, $S_3$ is turned off, $S_0$, $S_1$, $S_2$ are turned on. $D_3$ is forward biased. $V_1$ and $V_2$ charge inductors $L_1$ and $L_2$. Capacitor, $C_o$ supplies the load. In mode 3, $S_0$, $S_1$, $S_3$ and $D_2$ are turned on while $D_3$ is turned off. In mode 4, $S_2$ and $S_3$ are turned on while $S_0$ and $S_1$ are turned off. $D_o$ and $D_1$ are forward biased. $V_1$ delivers energy to the load.

The output voltage is given by:

$$V_o = \frac{V_1}{(1 - d_1)^2} + \frac{V_2}{1 - d_2} + \frac{V_3}{1 - d_3} \tag{25}$$

Modular structure and high VTR are the main advantages of this converter. There is also low voltage stress on switches. The drawback is the large parts count as the number of input increase.

Another modular high VTR converter, proposed by the same author in Ref. [125], made use of non-coupled inductors for each voltage source. The circuit is depicted in Fig. 13. The form is such that non-coupled inductor based single-input single-output (SISO) converters

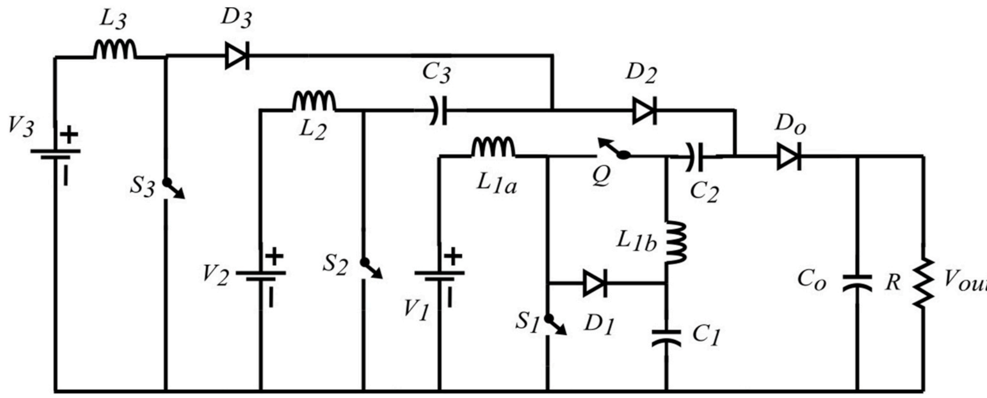


**Fig. 12.** Modular high VTR multi-input converter [124].

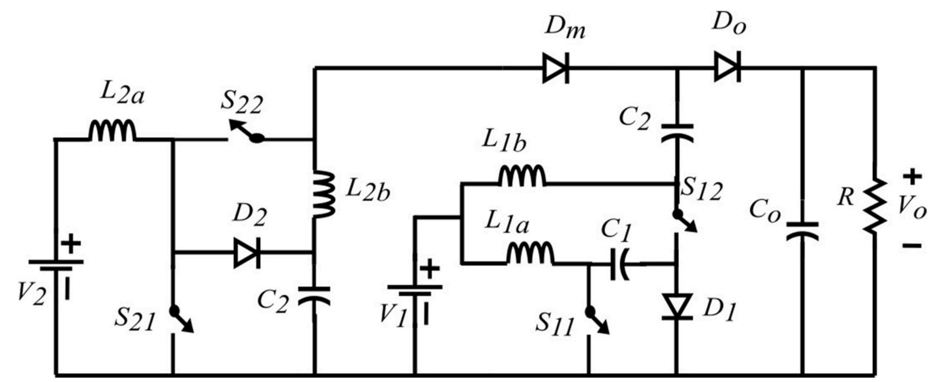


**Fig. 13.** Bidirectional modular high VTR multi-input converter [126].

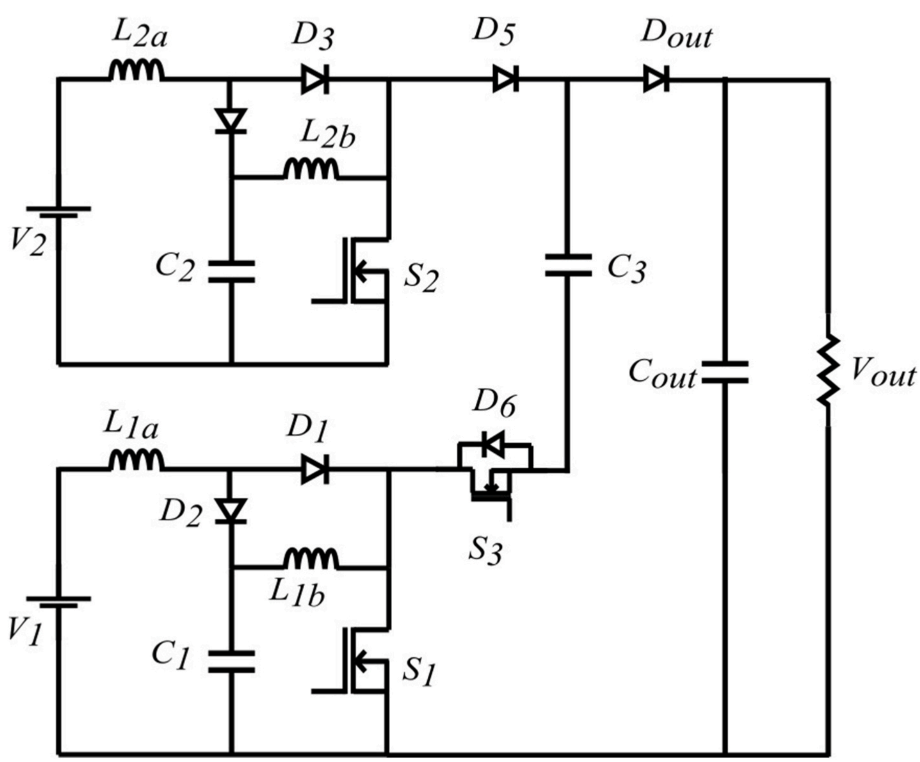


**Fig. 14.** High VTR multi-input converter with low average of normalised peak inverse voltage [127].

share a common filter and bidirectional switch. Each SISO module consists of three switches, two capacitors and two non-coupled inductors. The output voltage is given as:

$$V_o = V_1\frac{(2-d_1)}{(1-d_1)^2} + V_2\frac{1}{(1-d_2)^2} \quad (26)$$

In addition to the high gain of 25, the converter has low normalised voltage stress on the switches and bidirectional capability. There are less shared components implying that complexity of driving the SISO converters. There is high number of semiconductor devices as number of input sources increase. In Ref. [126], the current stress on the bidirectional switch for battery charging is quite high.

In [127], a voltage gain of 27.43 was achieved in a modular structure. In the converter, the duty ratio of the switches for individual units is independently assigned. Thus, with low duty ratio, voltage stresses are less. The topology is shown in Fig. 14. Each module has a modified switched inductor input. The converter has three operation modes as described hereafter.

Mode 1:

Switches $S_1$ and $S_2$ are turned on, diodes $D_1$, $D_3$ conduct. Capacitors $C_1$, $C_2$ are charged by the inductors, $L_{1a}$ and $L_{2a}$. The output capacitor, $C_{out}$ serves the load.

Mode 2:

Switch $S_1$ is turned off, $S_3$ is turned on an addition to already conducting $S_2$. Diodes, $D_2$ and $D_{out}$ are conducting. $V_2$ and $C_2$ charge $L_{2a}$ and $L_{2b}$ respectively. $L_{1b}$, $C_1$ and $C_3$ serve the load.

Mode 3:

Switch, $S_1$ is turned on. $S_2$ and $S_3$ are turned off. Diodes, $D_1$, $D_4$, $D_5$ and $D_6$ conduct. $V_1$ charges $L_{1a}$ and $C_1$ charges $L_{1b}$. $C_2$ and $L_{2b}$ charge $C_3$. $C_{out}$ supplies the load.

For the two-input converter model, the output voltage is given as:

$$V_o = V_1\frac{1}{(1-d_1)^2} + V_2\frac{1}{(1-d_2)^2} \quad (27)$$

In addition to the modular form, high voltage gain, and lower semiconductor device voltage stress, this converter has a lower average normalised peak inverse voltage. The high number of components is a shortcoming. Also, the duty ratio for power switches is high.

### 4.13. Multiple input and multiple output (MIMO) converter

In [128], the conventional resonant converter can be converted to multiple ports by attaching the desired port to a resonator connected to a forward-conducting bidirectional-blocking (FCBB) switch. This FCBB switch also helps to prevent short-circuiting of the ports. The topology is shown in Fig. 15. The topology adopted a switched-resonator converter architecture Each input and output port consist of a switch, a diode and resonant inductor. When $S_1$ is turned on, $Cr$ is charged to twice the value of $Vs_1$. Power delivery from $Cr$ to $V_{01}$ is possible when $S_3$ is turned on. It has the advantage of ZCS operation and power routing from point to point. Also, the addition of bidirectional ports can be conveniently done. A constraint of the converter is the increase count of magnetic elements and semiconductor devices as the number of input and output ports increases.

In [116], the converter is optimised for loads with different voltage requirements in EVs. Splitting of the outputs is achieved by using parallel switches in series with diodes. The value of $V_1$ must be higher than $V_2$ in the converter. $V_1$ is a fuel cell, whereas $V_2$ is a battery storage. The converter has two operating modes which are battery charging and battery discharging.

In [129], the authors used the conventional parallel connection of multiple inputs. For the multiple outputs, boost converter and SC are used.

In [130], the converter applied a mesh of buck-boost configuration and a matrix outlay. The power switches are crosswise, whereas the outputs are vertical thereby appearing like a matrix. All the outputs have an attached buck-boost converter formed with the attached output capacitor Although there is unlimited number of inputs, the outputs are not simultaneously powered by them. There is a high number of semiconductor devices in this converter.

The converter in Ref. [131] used the interleaved technique at the inputs and simple voltage divider outputs. This converter has a high component count.

In [132], the double inputs are a PV source and a battery storage. A conventional boost converter is attached for voltage gain. The converter has double outputs and bidirectional feature.

In [133], separate switching units, each with their output are cascaded. The presence of separate magnetic elements for the respective units implies that the output voltages are independent.

In [134], the SISO bidirectional buck-boost converter can be adapted for MIMO operation. To increment the input, a module consisting of an inductor in parallel with a half-bridge is placed on the boost side of the DC link capacitor. This modular structure implies that the output will increment when the module is positioned on the buck side of the DC-link capacitor. The converter is functional in the vehicle-to-grid interface.

Table 6 shows a summary of the properties of the electrically connected multi-input converters that have been critiqued.

## 5. Discussion, challenges and future research

### 5.1. Comparison and discussion

The respective categories of multi-input converters based on summaries in Table 1, Tables 2 and 6 are compared. It is observed that some converters possess two or more output voltage. This has to do with the respective operating condition, the value of input voltages or battery

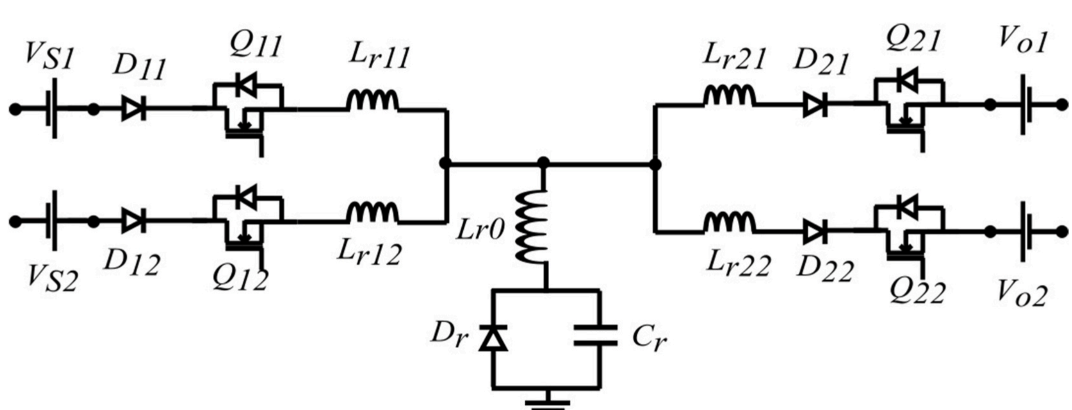


**Fig. 15.** Resonant multiple input and multiple output ZCS converter [128].

**Table 6**
Summary of electrically connected multi-input converters.

| Multi-input converter | Output voltage | S | D | L | C | Drawbacks |
|---|---|---|---|---|---|---|
| Series or parallel connected converter [58] | Series: $V_o = \frac{V_1}{1-d_1}+\frac{V_2}{1-d_2}$ | 4 | – | 2 | 2 | Difficult voltage regulation |
| [60] | Parallel: $V_o = \frac{V_1}{1-D_2} = \frac{V_2}{1-D_4} = \frac{V_3}{1-D_6}$ | | | | | Poor switch economy, no soft switching |
| Buck/buck-boost converter with double input [69] | $V_o = V_1\frac{d_1}{1-d_2}+V_2\frac{d_2}{1-d_2}$ | 2 | 2 | 1 | 1 | Limited output voltage, no battery charging |
| [67] | Series SC: $V_0 = V_1 + 2V_2$<br>Parallel SC: $V_o = \frac{3}{1-D}V_1$ | 2 | 3 | – | 4 | No battery charging |
| [71] | $V_o = \frac{V_1 d_1}{1-d_1-d_2} - \frac{V_2 d_2}{1-d_1-d_2}$ | 2 | 2 | 1 | 1 | No energy storage device |
| [76] | $V_o = V_1\frac{d_{s1}}{1-d_{To}} = V_2\frac{d_{s2}}{1-d_{To}}$ | 4 | 6 | 2 | 1 | |
| [79] | $V_o = D_1V_1 + D_2V_2$ | 3 | 6 | 1 | 2 | |
| [80] | $V_o = \frac{d_1V_1+d_2V_2}{1-d_1}$ | 2 | 3 | 1 | – | Voltage limit |
| [82] | $d_1 > d_2$: $V_o = \frac{2d_1-d_2}{(2-d_1)(2-d_2)}V_1 + \frac{d_2}{2-d_2}V_2$<br>$d_1 \le d_2$: $V_o = \frac{d_1}{(2-d_1)(2-d_2)}V_1 + \frac{d_2}{2-d_2}V_2$ | 2 | 8 | 3 | 3 | Efficiency not clarified |
| Double input SEPIC [87] | $V_o = V_1 d_1 + \frac{V_2 d_2}{1-d_2}$ | 2 | 4 | 2 | 1 | No battery charging |
| [89] | $V_o = \frac{V_{b1}d_1 + V_{b2}d_2}{(1-d_3)}$ | 4 | 4 | 1 | 1 | High switch voltage stress |
| Multi-input buck-boost converter [98] | $D_1 > D_2$: $V_o = \frac{2D_1}{1-d_1}V_1$<br>$D_2 > D_1$: $V_o = \frac{D_1V_1+(D_2-D_1)V_2}{1-D_2}$ | 2 | 1 | 1 | 1 | Negative output voltage, no simultaneous power delivery |
| [99] | $V_o = \frac{D_1V_1+(D_2-D_1)V_2}{1-D_2}$ | 5 | 3 | 1 | 1 | Limited power delivery |
| Switched capacitor based converter [100] | $V_o = V_1 + V_2 + V_3$ | 3 | 5 | – | 3 | High output ripple and output leakage voltage |
| [101] | $V_o = V_0 - V_1 - V_2$ | | | | | |
| Three-level switched-capacitor based converter [102] | $V_o = \frac{3V_{1,2}}{1-D_{1,2}-D_3}$ | 4 | 9 | 2 | 5 | High parts count |
| Converter based on switched inductor [104] | $V_o = \sum_{j=1}^{n}\frac{1+md_j}{1-d_j}(E_j + \propto E_{bat}$ | 4 | 14 | 4 | 3 | High number of components |
| Buck/boost-boost based multi-input converter [106] | $V_0 = \frac{V_2}{1-D_2} + \frac{D_1D_2}{(1-D_1)(1-D_2)}$ | 2 | 2 | 2 | 2 | High switch voltage and current ratings |
| Three switches leg based multiple input converter [107] | – | 6 | 6 | 2 | 1 | No soft switching, modulation index limitation |
| ZVS dual input converter [108] | $V_0 = \frac{(1-d_1)}{1-d_{dcm}-d_1}.\frac{1}{1-d_1}V_1$ | 3 | 1 | 3 | 1 | High semiconductor voltage stress |
| Three input boost converter for RE sources and battery [112] | PV and Battery: $V_o = \frac{V_1+d_4V_3}{1-d_2-d_4}$<br>PV, FC and Battery: $V_o = \frac{V_2+d_3V_3}{1-d_2-d_3}$ | 4 | 4 | 4 | 1 | Uncontrolled battery charge and discharge |
| [105] | $\frac{V_o}{V_{1,2}} = \frac{1+D^2-D}{(1-D)^2}$ | 4 | 8 | 2 | 2 | Increased loss due to number of passive elements |
| Bridge type dual input converter [118] | Buck: $V_o = V_1d_1 + V_2d_2 + (V_1 + V_2)d_3$<br>Buck-boost: $V_o = \frac{V_1d_1+V_2d_2+(V_1+V_2)d_3}{1-d_1-d_2-d_3}$<br>Boost: $V_o = \frac{V_1(d_1+d_3)+V_2(1-d_1)}{1-d_1-d_3}$ | 4 | 2 | 1 | 1 | High switch stress and ripples |
| High VTR converter with VM [120] two-input structure | $V_o = 3\frac{V_1}{(1-d_1)} + 2\frac{V_2}{(1-d_2)}$ | 2 | 7 | 2 | 5 | Low efficiency, no energy storage device |
| [122] three-input structure | $V_o = \frac{1}{1-d_1}V_1 + \frac{2}{1-d_2}V_2 + \frac{2}{1-d_3}V_3$ | | | | | |
| [123] n-input | $V_o = \frac{n+1}{2}\left(\frac{V_2}{1-D_2}+\frac{V_2}{1-D_1}\right)$ | 2 | 8 | 2 | 5 | No energy storage device |
| Modular high VTR multi-input converter [125] | $V_o = \frac{V_1}{(1-d_1)^2} + \frac{V_2}{1-d_2} + \frac{V_3}{1-d_3}$ | 4 | 4 | 4 | 4 | Incremental component count as inputs increase, no energy storage device |
| [125] | $V_o = V_1\frac{(2-d_1)}{(1-d_1)^2} + V_2\frac{1}{(1-d_2)^2}$ | 7 | 1 | 4 | 4 | |
| [127] | | 3 | 7 | 4 | 4 | High duty ratio for power switches |
| Multiple input and multiple output converter [130] | $V_o = \sqrt{\frac{0.5.T.R_l}{L}\sum_{i=1}^{n}V_iD_i}$ | 9 | 3 | 3 | 3 | Outputs are not simultaneously powered |
| [116] | – | 4 | 4 | 1 | 2 | |
| [129] | – | 3 | 8 | 1 | 5 | |

(continued on next page)

**Table 6** (*continued*)

| Multi-input converter | Output voltage | S | D | L | C | Drawbacks |
|---|---|---|---|---|---|---|
| [128] | – | 4 | 8 | 5 | – | |
| [131] | – | 6 | 9 | 2 | 3 | |
| S = switch, D = diode, L = inductor, C = capacitor | | | | | | |

charge/discharge mode. Careful evaluation reveals that the voltage gain of electrically connected multi-input converters is dependent on the duty ratio of the switches. For magnetically connected multi-input converters, the properties of the transformer winding like the number of turns determine the voltage transfer ratio. In electromagnetically connected converters, the transformer specifications play a significant role in the output voltage however, duty ratio of switches also influences the output voltage depending on the design. Thus, the electromagnetically connected converters have added advantage of higher voltage gain when contrasted with the other converter types.

The number of switches, diodes and passive elements used in the converters depends on the properties of the converter. For electrically connected multi-input converters, the less sophisticated converters have marginally lower semiconductor and passive element count. For example, the dual bridge-type converter has lower device count compared to the modular high step-up non-isolated converter. The semiconductor and passive elements count in magnetically connected multi-input converters is highest when correlated to the other types. This implies that the converter cost for the magnetically connected category is highest. By having the lowest number of semiconductors and passive elements, the electrically connected category has the lowest converter cost.

Table 7 presents the properties of multi-input converters classified for easy identification. In the table, the six characteristics are;

- degree of isolation.
- simultaneous power delivery.
- battery charging.
- soft switching.
- ability to deliver both DC and AC output.
- high voltage gain.

Isolated multi-input converters have been categorised as either magnetically connected multi-input converters or electromagnetically connected multi-input converters. The magnetically connected multi-input converters have all the input ports on the primary side isolated from one another in addition to the basic isolation between the load and the source. Apart from the primary advantage of separation between the input and output, the input ports can load different voltage values. Hence, including isolation during design should not be compulsory. It should depend on the peculiarities of the desired converter. The electromagnetically connected multi-input converters possess the basic isolation between input and output but do not possess isolation between all input ports. Recent research has succeeded in incorporating isolated and non-isolated output ports. This suggests more expensive converters with increased size.

**Table 7**
Characteristics of multi-input DC-DC converters.

| Converter | Isolation | Simultaneous power delivery | Battery charging | Soft switching | DC & AC output | High voltage gain |
|---|---|---|---|---|---|---|
| Multi-input converter with buck-boost configuration [6] | ✓ | | | | | |
| Double input full-bridge converter [10] | ✓ | ✓ | | ✓ | | |
| Bidirectional multiport converter [18] | ✓ | ✓ | | | | |
| Bidirectional multiport resonant converter [25] | ✓ | ✓ | | ✓ | | |
| Full bridge based on distributed transformer [33] | ✓ | | | | | |
| Three port half-bridge converter [34] | ✓ | ✓ | ✓ | | | |
| Combined DC link and transformer [36] | ✓ | ✓ | ✓ | ✓ | | |
| Boost-integrated full-bridge converter with phase-shift for three port interface [38] | ✓ | ✓ | ✓ | ✓ | | |
| Tri-modal bridge converter [41] | ✓ | | ✓ | | | |
| Converter with wide input voltage range using full bridge [51] | ✓ | | ✓ | | | |
| Multiport simultaneous power management converter [44] | ✓ | ✓ | | | | |
| Multi-input three-level converter [45] | ✓ | ✓ | | | | |
| Three-port converter for PV-battery [46] | ✓ | ✓ | ✓ | ✓ | | |
| Converter with DC and AC output [47] | ✓ | ✓ | | | ✓ | |
| ZCS boost converter [48] | ✓ | ✓ | | ✓ | | |
| High gain multi-input converter [40] | ✓ | ✓ | | | | ✓ |
| Bidirectional converter with multiple combinational battery storage inputs [52] | ✓ | ✓ | ✓ | | | |
| Series or parallel connected converter [58] | | ✓ | | | | |
| Buck/buck-boost converter with double input [69] | | ✓ | | ✓ | | |
| SEPIC/Cuk based double input converter [71] | | ✓ | | | | |
| Battery coupled double input buck-boost converter [76] | | ✓ | ✓ | | | |
| Multi-input buck-boost converter [98] | | Buck mode only | | | | |
| Switched capacitor based converter [100] | | | | ✓ | | |
| Series or parallel switched-diode-capacitor boost converter [67] | | ✓ | | | | |
| Multi-level switched-capacitor based converter [102] | | ✓ | | | | |
| Converter based on switched inductor [104] | | ✓ | ✓ | | | ✓ |
| Buck/boost-boost based multi-input converter [106] | | ✓ | | | | |
| Three switches leg based multiple input converter [107] | | ✓ | | | ✓ | |
| ZVS dual input converter [108] | | ✓ | | ✓ | | ✓ |
| Three input boost converter for RE sources and battery [112] | | ✓ | ✓ | | | |
| Bridge type dual input converter [117] | | ✓ | | | | |
| High VTR multi-input converter [125] | | ✓ | | | | ✓ |
| Multi-input multi-output converter [130] | | ✓ | ✓ | | | |

 

The input voltage sources of a multi-input converter should be able to serve the load individually and simultaneously. Increasing the number of input ports in the magnetically connected converter involves adding multi-winding transformers. Control in this converter is much more complicated. Electromagnetically connected converters majorly employ a common DC link on the primary side of the transformer. In electrically connected multi-input converters, several solutions have been proposed for the primary challenge of individual and simultaneous power delivery. Some solutions are by inserting PSCs with the proper network, series or parallel connection of converters, and cascading.

There is much emphasis on including optimal battery charge/discharge capability as evident in the three-input converter for PV/FC/battery applications and the battery integrated high step-up converter. The presence of battery charging in a grid system is imperative as the periods of bumper availability of irregular RE sources must be harnessed with the aid of battery storage. Also, this feature is a necessity in HEVs to supply the bidirectional port.

Soft-switching techniques are employed majorly in isolated converters. It is aimed at operating the converter at high frequency and reducing size/switching loss of the converter.

Current research trend focused on producing high voltage gain in electrically connected multi-input converters. Due to the unstable behaviour of converters when the duty ratio approaches unity, it is a target that high gain converters have low duty ratios, high efficiency and power density. Combination or tweaking of several established techniques like cascading converters and the use of VMs in electrically connected converters show promising results. A new feature of a standalone non-isolated converter that can deliver both AC and DC outputs without the need for an external inverter is also a prospect for the future. This requires more efforts aimed at better modulation and reducing switching losses.

An examination of the state-of-the-art in this work depicts the progress from series or parallel connection of converters to PVSC inputs and cascaded/modular multi-input converters in electrically connected converters. In such modular converters, an extra input is executed by adding a module. Major investigations focused on adding or improving desirable converter properties. Techniques like VM, SC, switched/coupled inductors, aimed at achieving high voltage gain in the converters have been implemented to assist the low output voltage of RE sources. Due to size and control complexity, magnetically connected multi-input converters rarely find application except where isolation is overly necessary.

From the literature, multi-input DC-DC converter topologies are linked to HEVs and RE systems in different ways. Generally, voltage levels of available energy sources are insufficient for proper operation of HEVs and RE systems. Consequently, all proposed topologies are designed to achieve step up and/or step-down operation. HEVs utilise two or more RE sources in order to achieve propulsion. The challenges faced by RE sources as highlighted in the introduction, imply that RE systems also require more than one energy source for optimal power generation. Hence, in the HEVs and RE systems, the multi-input DC-DC converter serves as a common denominator to reduce the potential high cost and complex operation if the respective energy sources are connected to separate SISO converters.

Bi-directional multi-input converters function in both HEVs and RE power generation systems. An input port with energy storage capability is used to achieve different objectives in such set-up. For HEVs, deceleration and regenerative braking produced energy that can be stored in the battery or UC. In addition, some systems enable energy transfer from vehicles to the electric grid and back. In situations where surplus energy is generated in standalone RE systems, the multi-input topologies ensure the bidirectional battery port can store such excess energy. In grid-connected scenario, surplus energy from the grid can be routed to the storage input port.

An examination of the energy sources recommended for each converter in Table 8 confirm solar energy, wind turbines and FC are the

**Table 8**
Typical industry application of selected multi-input DC-DC converters.

| Converter/Author | Recommended Energy source (s) | Typical Industry Application | Power Range |
|---|---|---|---|
| Multi-input converter with buck-boost configuration [6] | PV, commercial AC line. | RE power generation | >100 kW |
| Double input full-bridge converter [10] | PV, wind, and FC | RE power generation and uninterrupted power supply | |
| Current fed three-port bidirectional converter [11] | FC and battery | To provide power to telecommunication stations | |
| Quad-active bridge converter [12] | PV and battery | Used to integrate distributed generators and storage into high voltage AC distribution line | >100 kW |
| High frequency transformer based converter [13] | FC and battery | Electric vehicles | |
| Full bridge converter with high power efficiency [14] | PV | Standalone power generation | |
| Bidirectional multiport converter [18] | Fuel cell, PV, battery storage | RE power generation | |
| ZVS bidirectional converter [20] | Battery and UC | Integration into DC distribution line | 6–9 kW |
| Liu et al. [21], | PV and battery | Standalone PV lighting system | 1 kW |
| Phattanasak et al. [22], | FC and supercapacitor | Can provide power for small EVs | 35 kW |
| Jakka et al. [23], | PV, FC, wind and battery | DC microgrid | 15 kW |
| Tomas-Manez et al. [24], | PV and battery | For integration of distributed generators to grid-tied inverters | 1–4 kW |
| Bidirectional multiport resonant converter [25] | PV, battery, ultracapacitor | DC grids, HEV | 7–44 kW |
| Wang et al. [31], | Battery, UC and supercapacitor | Grid connected RE power generation | 1–10 kW |
| Full bridge based on distributed transformer [33] | PV, wind, fuel cell | Hybrid RE system | >100 kW |
| Three port half-bridge converter [34] | PV and battery | Standalone RE power generation | |
| Combined DC link and transformer [36] | Fuel cell and super capacitor | HEV power train, bidirectional power generation for microgrid | 35 kW |
| Interleaved half bridge three port converter [37] | PV and battery | RE power generation system | 1–5 kW |
| Boost-integrated full-bridge converter with phase-shift for three port interface [38] | PV and battery | Power source for satellite system | 1.5–5 kW |
| Al-Atrash et al. [39], | Battery, UC and Supercapacitor | Can be used to integrate backup to microgrid | 1–5 kW |
| Tri-modal bridge converter [41] | PV and battery | Power for satellite applications | 2 kW |
| Qian et al. [43], | PV, wind and battery | Low power RE harvesting | 500 W |
| Converter with wide input voltage range using full bridge [51] | PV and battery | Communication systems traffic lights | |
| | PV and wind | | |

(continued on next page)

**Table 8** (*continued*)

| Converter/Author | Recommended Energy source (s) | Typical Industry Application | Power Range |
|---|---|---|---|
| Multiport simultaneous power management converter [44] | | Hybrid power generation system | |
| Multi-input three-level converter [45] | PV, wind, fuel cell | Low power generation for domestic use | |
| Three-port converter for PV-battery [46] | PV and battery | Satellite power supply | 1–2 kW |
| Converter with DC and AC output [47] | Fuel cell or PV | Residential RE power supply. Converter has dedicated AC and DC output ports. | 1 kW |
| ZCS boost converter [48] | PV and wind | Hybrid standalone power system | |
| Reddi et al. [49], | PV and wind | Produces AC voltage at the output. Can be used for direct integration of RE sources to power local AC loads. | 3 kW |
| Lin et al. [50], | PV and battery | Standalone power generation for domestic use | 1 kW |
| High gain multi-input converter [40] | PV | DC microgrid | |
| Converter with combinational battery storage inputs [52] | Battery | RE fed DC distribution grid | |
| Non-isolated Series-connected converter [58] | Wind and PV | RE power generating system | 10 kW |
| Imes and Rodriguez [59] | PV and battery | Low power management in spacecrafts and satellites | 150–400 W |
| Non-isolated Parallel connected converter [61,62] | FC, UC and battery | HEV power generation and storage | 60 kW |
| Zhang et al. [63], | PV and battery | Can be used to interface multiple distributed DC sub-systems | 1–2 kW |
| Chen et al. [66], | PV and wind | Battery charging | 1.5 kW |
| Buck/buck-boost converter with double input [69] | PV and wind | RE power generation for domestic use | 1 kW |
| SEPIC/Cuk based double input converter [70] | PV and battery | Standalone low power generation and storage for domestic use | 500 W |
| Battery coupled double input buck-boost converter [76] | FC, UC, PV and battery | HEVs and DC microgrids | |
| Sun et al. [79], | FC and battery | RE power system with high fault tolerance requirement | 1–3 kW |
| Park and Kim [80] | PV | To power traffic lights | 300 W |
| Muntean et al. [86], | PV, wind and battery | Can be applied in both standalone and grid connected RE systems | 1–3 kW |
| Moury et al. [90], | PV and wind | Wind-solar energy system | 1 kW |
| Haghighian et al. [94], | PV, wind and battery | Street lighting | 2 kW |
| Wai and Hong [97] | PV, micro-hydro, geothermal and battery | Standalone power generation from low RE sources | 1.5–3 kW |
| Khaligh and Cao [99] | PV, wind and battery | Provide/store power to/from DC microgrid | 3 kW |
| Multi-input buck-boost converter [98] | FC, UC and battery | HEVs | 35 kW |
| Switched capacitor based converter [100] | PV | Traffic light, low power electronics | 500 W |
| Series or parallel switched-diode-capacitor boost converter [67] | PV and FC | Uninterrupted power supply, domestic power generation | |
| Multi-level switched-capacitor based converter [102] | FC, PV and battery | DC microgrid | |
| Converter based on switched inductor [104] | PV, FC, wind and battery | Smart grid connected with distributed generators | |
| Buck/boost-boost based multi-input converter [106] | PV | Standalone power generation | |
| Three switches leg based multiple input converter [107] | PV, FC, wind and battery | Converter can function as an inverter, grid-connected application | |
| ZVS dual input converter [108] | FC and battery | Provision of constant DC source for motor drives. Can serve scooters and electric bikes | 800 W |
| Wai et al. [109], | FC and battery | Deliver power to microgrid | 5–10 kW |
| Mohammadi and Moghani [110] | Battery and supercapacitor | Two-way power delivery in DC microgrid | 6 kW |
| Three input boost converter for RES and battery [112] | PV, FC and battery | Standalone power generation | |
| Ghavidel et al. [114], | PV, FC and battery | RE microgrid | 8 kW |
| Balaji et al. [115], | PV, FC and battery | Power drive train of EVs | 60 kW |
| Nahavandi et al. [116], | FC and battery | Can be used to provide different voltage levels to electric motor and cabin ventilation units. Converter possesses multiple output ports | 60 kW |
| Bridge type dual input converter [117] | Supercapacitor and battery | Electric vehicle, uninterrupted power supplies | 60 kW |
| High gain converter based on VM cells [120] | PV, FC and geothermal source | Can be used to draw continuous current in RE system like solar farm | 400 V DC bus, 1–10 kW |
| Mohseni et al. [122], | PV and FC | Can be used to deliver more than one high voltage output as needed | 5–10 kW |
| Zhu et al. [123], | PV | Low cost solar power generation | 2 kW |
| High VTR multi-input converter [125] | PV, FC, and battery | Grid connected microgrids | |
| Mohammadi et al. [127], | PV and wind | Standalone RE power generation | 1.5 kW |
| Babaei and Abbasi [129] | PV and FC | Multiple DC voltage levels for telecom base stations. | 5 kW |
| Multi-input multi-output converter [130] | FC, PV, and wind | Can be used to integrate RE sources or charge a battery | 1 kW |
| Gorji et al. [131], | PV and battery | Provide two different voltage levels for satellite communication systems | 1.5 kW |
| Saeed et al. [132], | PV and battery | HEV charging and discharging | |
| Khan et al. [133], | | Used to interface with DC microgrid | |
| Khan et al. [134], | FC, SC, and battery | Can be used for vehicle charging and bidirectional vehicle to grid energy transfer | 9–60 kW |

most sought after RE sources for application in the industry. Due to size and dependence on wind speed/air density of location, wind turbines find utility principally in power generation for standalone RE system or microgrid. PV cells, in addition to providing power for microgrids, can be adapted for satellite power, communication equipment and specialised HEV/ships. Portability is one advantage for FC in HEVs and spacecrafts. Geothermal RE sources do not have the advantage of portability, thus restricting them to providing electricity for standalone and grid usage.

Although unidirectional multi-input converter topologies majorly find application in standalone RE power generation systems, some HEV and spacecraft utilise such converter to power secondary system like ventilation. In such RE power generation system where a storage device is non-existent, each energy source can be connected to a PVSC input before a common step up/step down segment and filter to the output port. For energy storage devices to exist in a multi-input converter, the converter must have at least one bidirectional port. In such bidirectional converters, the most used storage devices are batteries, UC and the supercapacitor. HEVs operate better with UC or supercapacitor as storage device during regenerative braking or acceleration due to fast charge and discharge property. Battery banks frequently serve in conjunction with PV, wind turbine and/or geothermal plant.

In the industry, real life applications of multi-input converters as identified in Table 8 show that this area of study has matured from series/parallel connection of several converters in the early days to sophisticated multi-input converters that are have the capability to provide different types of output voltage. Worthy of note is the multi-input converter that can simultaneously deliver DC and AC voltage output. Such converter is invaluable to the operation of battery EVs, plug-in HEVs and fast charging stations that require high power rating.

It is vital to clarify the bidirectional operation of a multi-input converter with respect to industry application. In a two-input converter for HEV operation, the bidirectional converter must allow backward power flow from the high voltage port to one or both low voltage port. The same operation is imperative for a grid-connected two input converter. Surplus energy from the grid can thus be channelled to a battery bank. In the cases, power rating for the multi-input converters is in the range of 60 kW for HEV and over 100 kW for grid-connected system. The multi-input converter has a bidirectional port but cannot allow backward flow from high voltage port to low voltage ports. The operation is such that surplus energy from the other RE sources is channelled to the bidirectional port with attached energy storage device. Such converter should deliver high power density. To draw continuous high current from the RE sources, the current-fed topology should be considered. The converter can serve in standalone power generation, DC microgrids, telecommunication sub-stations and satellite system.

The choice of a multi-input converter should take into consideration the specific purpose. For example, multi-input converter dedicated to battery charging will have no need for a bidirectional port. Similarly, multi-input converters for traffic light and signalling installations do not need high power rating. A converter for DC microgrid can be designed to exhibit a high level of fault tolerance in order to mitigate short circuits. Converter designers may decide to combine topologies as deemed fit to achieve desired objectives but should attempt to limit the effects of the drawbacks of chosen topologies.

### 5.2. Challenges and future research

This review of the literature identified the constraints faced by multi-input converters. These constraints should influence the design choices as regards the suitability of a converter for an application. There is the problem of converters having low efficiency. Such converter experience high losses that may arise from switches, conduction material or copper losses in the isolating transformer. Soft switching at high frequency can aid improvement of the efficiency in addition to size reduction. Although two input ports are present, the converter cannot draw power simultaneously from the input ports. This absence of source utility implies that only one input source can service the output port at a determined time. The cost of the converter increased when large number of components in the converter especially with transformer winding, magnetic element semiconductor devices. Complex control problems mostly in isolated converter can result in zero voltage clamp. Some converters have voltage limitations, problematic voltage regulation and poor power sharing by input sources and load. These constraints described are dependent on the topology of the converter.

The function of an inverter positioned after the DC link in HEV or the DC bus in grid connected RE power generation is to convert the DC to AC in order to drive the power train in HEV or power AC mains in RE power generation. The topology proposed to eliminate this inverter from the setup experience low modulation index associated with the discontinuous conduction mode operation of the DC-DC component of the converter. The modulation index controls the AC output voltage hence at low modulation index, the corresponding AC output voltage will be low.

As researchers continue to investigate new topologies, another challenge that continue to arise is optimal control issue for both input voltages and output voltages. In industry applications that require several output voltages from the multi-input converter, usage of voltage divider output induces losses in the passive element. Parallel connection of a switch with a dedicated filtering capacitor implies that the duty cycle will control the output voltage. In this situation, switch stress will be high. As such, it is difficult to achieve the desired output parameters.

Consequently, future research focus should be on proposing new multi-input topologies that can efficiently deliver both DC and AC output voltages. Such converter will aid the reduction of installation cost and size by eliminating the original output inverter. In addition, increased efforts are required in the control of multiple output. Although several converters allow for wide input voltage ranges, there is room for improvement especially with respect to multi-input converters devoted to draw energy from very low RE sources. Future research on multi input converters may focus on simplification of the circuitry, reduction of the number of components, improvements of voltage gain and power scalability. Circuit simplification and reduction of components will result in lower costs of converters. Improvement of voltage gain will impact positively on converter output.

Finally, while fossil fuels still dominate the energy market, efforts to achieve one hundred percent renewable energy penetration will end in nullity if research on the power electronics is inadequate. It is therefore critical that research on issues like reliability, efficiency and power losses in multi-input converters be conducted.

## 6. Conclusion

The fundamental objective of the authors in this review, is to furnish readers with an updated status on research into the application of multi-input DC-DC converters in HEVs and RE systems. The multi-input converters play similar role in HEVs and RE systems. Primarily, the variable and irregular nature of RE sources encouraged interest in multi-input converters. These converters can reduce cost and handle control issues that may arise from connecting several converters to a common DC bus. The work done identified three classifications of multi-input converters. Based on isolation between the input ports and the output ports, the classes are; magnetically connected multi-input converters, electromagnetically connected multi-input converters and electrically connected multi-input converters. In magnetically connected converters, input ports are created by adding an extra winding on the low voltage side of the transformer. Some desired features in this type of converter are isolation, battery charging, high power rating and soft switching. The electromagnetically connected converters use a DC-link to add input ports before the transformer winding between the output and the inputs. Some advantages are bidirectional operation and lower cost than the magnetically connected converter. In electrically connected multi-input converters, there are no transformer windings, Thus, both input and output have a common ground via electrical means. Synthesis of electrically connected multi-input converters developed from series and parallel connection of converters to inclusion of PVSC units tied to energy sources. Example of several proposed topologies are cascaded inputs, three level inputs and current-fed inputs. Some desired features in these converters are high voltage gain, low losses, and multiple output voltage.

The operation of multi-input converters in industry ranges from HEVs and RE systems to battery chargers, uninterrupted power supplies, street lighting, traffic lights, telecommunication base stations, spacecrafts, satellite systems and microgrids. The converters for each application differ in power range as well as directional operation. For HEVs, bidirectional electrically connected multi-input converters with fuel cell and supercapacitor inputs are recommended. For microgrid power generation, three input bidirectional high gain electrically connected converters with PV, wind turbine and battery bank are recommended.

Finally, the constraints and challenges facing the respective converters have been identified. Although all converters exhibit some drawbacks, they can be used based on the conditions to be satisfied. Future research will aim to propose multi-input converters that have reduced cost, size and both AC and DC output with optimal control, while looking to better manage RE sources with improved efficiency.

### Declaration of competing interest

The authors declare that they have no known competing financial interests or personal relationships that could have appeared to influence the work reported in this paper.

### Acknowledgements

The authors acknowledge the support of RIMC, Universiti Malaysia Sarawak and the Ministry of Higher Education, Malaysia (FRGS/1/2017/TK10/UNIMAS/03/01) for this work. In addition, the authors would like to thank the respective copyright holders for permission granted to include cited graphics, images tables and/or figures in this work.

### References

[1] Reddy JK, Natarajan S. Energy sources and multi-input DC-DC converters used in hybrid electric vehicle applications – a review. Int J Hydrogen Energy 2018;43:17387–408.
[2] Lavanya A, Navamani JD, Vijayakumar K, Rakesh R. Multi-input DC-DC converter topologies-a review. In: 2016 international conference on electrical, electronics, and optimization techniques. ICEEOT); 2016. p. 2230–3.
[3] Khosrogorji S, Ahmadian M, Torkaman H, Soori S. Multi-input DC/DC converters in connection with distributed generation units – a review. Renew Sustain Energy Rev 2016;66:360–79.
[4] Yalamanchili KP, Ferdowsi M. Review of multiple input DC-DC converters for electric and hybrid vehicles. In: 2005 IEEE vehicle power and propulsion conference; 2005. p. 552–5.
[5] Rehman Z, Al-Bahadly I, Mukhopadhyay S. Multiinput DC-DC converters in renewable energy applications - an overview. Renew Sustain Energy Rev 2015;41:521–39.
[6] Matsuo H, Shigemizu T, Watanabe N, Kurokawa F. Characteristics of the multiple-input DC-DC converter. In: Proceedings of IEEE power electronics specialist conference - PESC '93. IEEE; 1993. p. 115–20.
[7] Matsuo H, Lin W, Kurokawa F, Shigemizu T, Watanabe N. Characteristics of the multiple-input DC-DC converter. IEEE Trans Power Electron 2004;51:625–31.
[8] Kobayashi K, Matsuo H, Sekine Y. Novel solar-cell power supply system using a multiple-input DC-DC converter. IEEE Trans Ind Electron 2006;53:281–6.
[9] Chen YM, Liu YC. Development of multi-port converters for hybrid wind-photovoltaic power system. Proceedings of IEEE region 10 international conference on electrical and electronic technology. IEEE; 2001. p. 804–8.
[10] Chen Yaow-Ming, Liu Yuan-Chuan, Wu Feng-Yu. Multi-input DC/DC converter based on the multiwinding transformer for renewable energy applications. IEEE Trans Ind Appl 2002;38:1096–104.
[11] Krishnaswami H, Mohan N. A current-fed three-port bi-directional DC-DC converter. Intelec 07 - 29th international telecommunications energy conferencee. INTELEC; 2007. p. 523–6.
[12] Falcones S, Ayyanar R, Mao X. A DC-DC Multiport-converter-based solid-state transformer integrating distributed generation and storage. IEEE Trans Power Electron 2013;28:2192–203.
[13] Zhigang G, Fenlin J. Isolated multi-port DC-DC converter based on a high frequency transformer. 18th international conference on electrical machines and systems. ICEMS; 2016. p. 564–8.
[14] Suetomi M, Matsuo H, Hirakida K, Nakkashima R, Hamaguchi R, Isizuka Y, et al. A novel multi-input DC-DC converter with high power efficiency. IEEE 33rd international telecommunications energy conference (INTELEC). IEEE; 2011. p. 1–5.
[15] Li Y, Zhao C, Chen JY, Du R, Zhang Y. Optimizing design of soft-switching dual-input full-bridge DC/DC converter. IEEE vehicle power and propulsion conference. 2011. p. 1–6.
[16] Yang D, Ruan X, Li Y, Liu F. Multiple-input full bridge DC/DC converter. IEEE energy conversion congress and exposition. IEEE; 2009. p. 2881–8.
[17] Mao H, Abu-Qahouq J, Luo S, Batarseh I. Zero-voltage-switching half-bridge DC-DC converter with modified PWM control method. IEEE Trans Power Electron 2004;19:947–58.
[18] Tao H, Kotsopoulos A, Duarte JL, Hendrix MAM. Family of multiport bidirectional DC–DC converters. IEE Proc Elec Power Appl 2006;153:451–8.
[19] Tao H, Duarte JL, Hendrix MAM. Three-port triple-half-bridge bidirectional converter with zero-voltage switching. IEEE Trans Power Electron 2008;23:782–92.
[20] Liu D, Li H. A ZVS bi-directional DC-DC converter for multiple energy storage elements. IEEE Trans Power Electron 2006;21:1513–7.
[21] Liu S, Zhang X, Guo H, Xie J. Multiport DC/DC converter for stand-alone photovoltaic lighting system with battery storage. International conference on electrical and control engineering. IEEE; 2010. p. 3894–7.
[22] Phattanasak M, Gavagsaz-Ghoachani R, Martin JP, Nahid-Mobarakeh B, Pierfederici S, Davat B. Control of a hybrid energy source comprising a fuel cell and two storage devices using isolated three-port bidirectional DC-DC converters. IEEE Trans Ind Appl 2015;51:491–7.
[23] Jakka VNSR, Shukla A, Demetriades GD. Dual-transformer-based asymmetrical triple-port active bridge (DT-ATAB) isolated DC-DC converter. IEEE Trans Ind Electron 2017;64:4549–60.
[24] Tomas-Manez K, Zhang Z, Ouyang Z. Multi-port isolated LLC resonant converter for distributed energy generation with energy storage. In: IEEE energy conversion congress and exposition. ECCE. IEEE; 2017. p. 2219–26.
[25] Tran YK, Dujic D, Barrade P. Multiport resonant DC-DC converter. In: Iecon 2015 - 41st annual conference of the IEEE industrial electronics society. IEEE; 2015. p. 3839–44.
[26] Tran Y, Freijedo FD, Dujic D. Open-loop power sharing of three-port DC-DC resonant converters. In: 2019 IEEE applied power electronics conference and exposition (APEC). IEEE; 2019. p. 2138–44.
[27] Tran Y, Freijedo FD, Dujic D. Open-loop power sharing characteristic of a three-port resonant LLC converter. CPSS Trans Power Electron Appl 2019;4:171–9.
[28] Tran YK, Dujic D. A multiport isolated DC-DC converter. In: 2016 IEEE applied power electronics conference and exposition (APEC). IEEE; 2016. p. 156–62.
[29] Tran YK, Dujic D. A multiport medium voltage isolated DC-DC converter. In: Iecon 2016 - 42nd annual conference of the IEEE industrial electronics society. IEEE; 2016. p. 6983–8.
[30] Liu R, Li Z. A three-port multi-element resonant converter with decoupled power flow management. In: IEEE 4th southern power electronics conference (SPEC). IEEE; 2018. p. 1–5.
[31] Wang Y, Han F, Yang L, Xu R, Liu R. A three-port bidirectional multi-element resonant converter with decoupled power flow management for hybrid energy storage systems. IEEE Access 2018;6:61331–41.
[32] Zhang Z, Thomsen OC, Andersen MAE, Nielsen HR. A novel dual-input isolated current-fed DC-DC converter for renewable energy system. Twenty-sixth annual IEEE applied power electronics conference and exposition (APEC). IEEE; 2011. p. 1494–501.
[33] Zhang Z, Thomsen OC, Andersen MAE, Nielsen HR. Dual-input isolated full-bridge boost dc–dc converter based on the distributed transformers. IET Power Electron 2012;5:1074–83.
[34] Wu H, Xing Y, Chen R, Zhang J, Sun K, Ge H. A three-port half-bridge converter with synchronous rectification for renewable energy application. IEEE energy conversion congress and exposition. IEEE; 2011. p. 3343–9.
[35] Wu H, Chen R, Zhang J, Xing Y, Hu H, Ge H. A family of three-port half-bridge converters for a stand-alone renewable power system. IEEE Trans Power Electron 2011;26:2697–706.
[36] Tao H, Kotsopoulos A, Duarte JL, Hendrix MAM. Multi-input bidirectional DC-DC converter combining DC-link and magnetic-coupling for fuel cell systems. In: Fourtieth IAS annual meeting conference record of the 2005 industry applications conference; 2005. 2021–8.
[37] Wu H, Sun K, Zhu L, Xing Y. An interleaved half-bridge three-port converter with enhanced power transfer capability using three-leg rectifier for renewable energy applications. IEEE J Emerg Sel Top Power Electron 2016;4:606–16.
[38] Al-Atrash H, Batarseh I. Boost-integrated phase-shift full-bridge converter for three-port interface. In: 2007 IEEE power electronics specialists conference; 2007. p. 2313–21.
[39] Al-atrash H, Pepper M, Batarseh I. A zero-voltage switching three-port isolated full-bridge converter. Intelec 06 - twenty-eighth international telecommunications energy conference. 2006. p. 1–8.
[40] Raizada S, Verma V. Isolated high gain multi-input converter fed floating PV system for DC microgrid. 13th IEEE international conference on industry applications (INDUSCON). IEEE; 2018. p. 312–8.
[41] Al-Atrash H, Tian F, Batarseh I. Tri-modal half-bridge converter topology for three-port interface. IEEE Trans Power Electron 2007;22:341–5.

[42] Qian Z, Abdel-Rahman O, Al-Atrash H, Batarseh I. Modeling and control of three-port DC/DC converter interface for satellite applications. IEEE Trans Power Electron 2010;25:637–49.
[43] Qian Z, Abdel-Rahman O, Batarseh I. An integrated four-port DC/DC converter for renewable energy applications. IEEE Trans Power Electron 2010;25:1877–87.
[44] Jianwu Z, Wei Q, Liyan Q, Jiao Y. An isolated multiport DC-DC converter for simultaneous power management of multiple different renewable energy sources. IEEE J Emerg Sel Top Power Electron 2014;2:70–8.
[45] Dusmez S, Li X, Akin B. A new multiinput three-level DC/DC converter. IEEE Trans Power Electron 2016;31:1230–40.
[46] Zhu H, Zhang D, Athab HS, Wu B, Gu Y. PV isolated three-port converter and energy-balancing control method for PV-battery power supply applications. IEEE Trans Ind Electron 2015;62:3595–606.
[47] Kishore PM, Bhimasingu R. Boost multi-port converter with simultaneous isolated DC, non-isolated DC and AC outputs. Iecon 2018 - 44th annual conference of the IEEE industrial electronics society. 2018. p. 1061–6.
[48] Nareshkumar R, Gawande SP, Koteswararao K, Ramteke MR, Suryawanshi HM. Multiport DC-DC boost converter with zero current switching. IEEE international conference on power electronics, drives and energy systems (PEDES). IEEE; 2016. p. 1–6.
[49] Reddi NK, Ramteke MR, Suryawanshi HM, Kothapalli K, Gawande SP. An isolated multi-input ZCS DC-DC front-end-converter based multilevel inverter for the integration of renewable energy sources. IEEE Trans Ind Appl 2018;54:494–504.
[50] Lin X, Jia Y, Tian J, Ren C, Wang J, Wang P, et al. Partly-isolated four-port converter based on bidirectional full-bridge DC/DC converter. 13th IEEE conference on industrial electronics and applications (ICIEA). IEEE; 2018. p. 287–92.
[51] Wu H, Sun K, Chen R, Hu H, Xing Y. Full-bridge three-port converters with wide input voltage range for renewable power systems. IEEE Trans Power Electron 2012;27:3965–74.
[52] Karthikeyan V, Gupta R. Multiple-input configuration of isolated bidirectional DC-DC converter for power flow control in combinational battery storage. IEEE Trans Ind Informatics 2018;14:2–11.
[53] Kwasinski A. Identification of feasible topologies for multiple-input DC-DC converters. IEEE Trans Power Electron 2009;24:856–61.
[54] Liu YC, Chen YM. A systematic approach to synthesizing multi-input DC-DC converters. IEEE Trans Power Electron 2009;24:116–27.
[55] Kumar L, Jain S. A multiple source DC/DC converter topology. Int J Electr Power Energy Syst 2013;51:278–91.
[56] Li Y, Ruan X, Yang D, Liu F, Tse CK. Synthesis of multiple-input DC/DC converters. IEEE Trans Power Electron 2010;25:2372–85.
[57] Chen G, Jin Z, Deng Y, He X, Qing X. Principle and topology synthesis of integrated single-input dual-output and dual-input single-output DC-DC converters. IEEE Trans Ind Electron 2018;65:3815–25.
[58] Solero L, Caricchi F, Crescimbini F, Honorati O, Mezzetti F. Performance of A 10 kW power electronic interface for combined wind/PV isolated generating systems. PESC record 27th annual IEEE power electronics specialists conference. IEEE; 1996. p. 1027–32.
[59] Imes WG, Rodríguez FD. A two-input tri-state converter for spacecraft power conditioning. Intersociety energy conversion engineering conference. IEEE; 1994. p. 163–8.
[60] Rodriguez FD, Imes WG. Analysis and modeling of a two-input DC/DC converter with two controlled variables and four switched networks. IECEC 96 proceedings of the 31st intersociety energy conversion engineering conference. IEEE; 1996. p. 322–7.
[61] Di Napoli A, Crescimbini F, Rodo S, Solero L. Multiple input DC-DC power converter for fuel-cell powered hybrid vehicles. In: IEEE 33rd annual IEEE power electronics specialists conference. IEEE; 2002. p. 1685–93.
[62] Solero L, Lidozzi A, Pomilio JA. Design of multiple-input power converter for hybrid vehicles. IEEE Trans Power Electron 2005;20:1007–16.
[63] Zhang J, Wu H, Huang J, Xing Y, Ma X. A novel multi-port bidirectional converter for interfacing distributed DC micro-grid. In: IEEE 23rd international symposium on industrial electronics (ISIE). IEEE; 2014. p. 2344–8.
[64] Majumder R, Bag G. Parallel operation of converter interfaced multiple microgrids. Int J Electr Power Energy Syst 2014;55:486–96.
[65] Wu H, Zhang J, Xing Y. A family of multiport buck-boost converters based on DC-link-inductors (DLIs). IEEE Trans Power Electron 2015;30:735–46.
[66] Chen CW, Liao CY, Chen KH, Chen YM. Modeling and controller design of a semiisolated multiinput converter for a hybrid PV/wind power charger system. IEEE Trans Power Electron 2015;30:4843–53.
[67] Hou S, Chen J, Sun T, Bi X. Multi-input step-up converters based on the switched-diode-capacitor voltage accumulator. IEEE Trans Power Electron 2016;31: 381–93.
[68] Jananie C, Rajambal K. Multi-input high step-up converter using switched-diode-capacitor. In: 2017 international conference on power and embedded drive control. ICPEDC); 2017. p. 229–34.
[69] Chen YM, Liu YC, Lin SH. Double-input PWM DC/DC converter for high-/low-voltage sources. IEEE Trans Ind Electron 2006;53:1538–45.
[70] Kanhav KA, Chaudhari MA. Experimental realization of a multi-input buck–boost DC–DC converter. Turk J Electr Eng Comput Sci 2018;26:1453–69.
[71] Kanhav KA, Chaudhari MA. A reliable multiple input DC-DC converter for hybrid power system. In: 2017 second international conference on electrical, computer and communication technologies. ICECCT); 2017. p. 1–7.
[72] Yalamanchili KP, Ferdowsi M, Corzine K. New double input DC-DC converters for automotive applications. In: IEEE vehicle power and propulsion conference. IEEE; 2006. p. 1–6.
[73] Gummi K, Ferdowsi M. Synthesis of double-input DC-DC converters using a single-pole triple-throw switch as a building block. In: 2008 IEEE power electronics specialists conference; 2008. p. 2819–23.
[74] Gummi K, Ferdowsi M. Derivation of new double-input dc-dc converters using H-bridge cells as building blocks. In: 2008 34th annual conference of IEEE industrial electronics; 2008. p. 2806–11.
[75] Prabhala VAK, Somayajula D, Ferdowsi M. Power sharing in a double-input buck converter using dead-time control. In: 2009 IEEE energy conversion congress and exposition. IEEE; 2009. p. 2621–6.
[76] Akar F, Tavlasoglu Y, Ugur E, Vural B, Aksoy I. A bidirectional nonisolated multi-input DC-DC converter for hybrid energy storage systems in electric vehicles. IEEE Trans Veh Technol 2016;65:7944–55.
[77] Vural B. FC/UC hybridization for dynamic loads with a novel double input DC-DC converter topology. Int J Hydrogen Energy 2013;38:1103–10.
[78] Akar F, Tavlasoglu Y, Vural B. Analysis and experimental verification of a multi-input converter for DC microgrid applications. IET Power Electron 2018;11: 1009–17.
[79] Sun X, Zhou Y, Wang W, Wang B, Zhang Z. Alternative source-port-tolerant series-connected double-input DC-DC converter. IEEE Trans Power Electron 2015;30: 2733–42.
[80] Park J, Kim J. A non-isolated dual-input DC-DC converter with wide input voltage range for renewable energy sources. In: IEEE 3rd international future energy electronics conference and ECCE asia. IEEE; 2017. p. 654–8.
[81] Muntean N, Gavris M, Cornea O. Dual input hybrid DC-DC converters. In: IEEE EUROCON - international conference on computer as a tool. IEEE; 2011. p. 1–4.
[82] Gavris M, Muntean N, Cornea O. A new dual-input hybrid buck DC-DC converter. In: International aegean conference on electrical machines and power electronics and electromotion, joint conference. IEEE; 2011. p. 109–14.
[83] Gavris M, Cadariu L, Caruntu B, Cornea O, Muntean N. Analysis of the dual input hybrid buck DC-DC converter in boundary conduction mode. In: International conference on optimization of electrical and electronic equipment (OPTIM). IEEE; 2014. p. 601–6.
[84] Gavris M, Cornea O, Muntean N. Dual input hybrid buck LC converter. In: International symposium on power electronics power electronics, electrical drives, automation and motion. IEEE; 2012. p. 309–14.
[85] Cornea O, Muntean N, Teodorescu R, Gavris ML. Dual input hybrid buck LC converter for a mixed wind and PV array generation system. In: 15th international power electronics and motion control conference (EPE/PEMC). IEEE; 2012. p. 1–6.
[86] Muntean N, Gavris M, Cornea O. Dual input, small power, PV and wind energy conversion system. In: 13th international conference on optimization of electrical and electronic equipment (OPTIM). IEEE; 2012. p. 906–11.
[87] Veerachary M. Buck-integrated SEPIC converter for photovoltaic power conversion. In: Intelec 2009 - 31st international telecommunications energy conference. IEEE; 2009. p. 1–5.
[88] Kumar EV, Veerachary M. Steady-state analysis of large step-down ratio two-input DC-DC converter. In: International conference on control communication and computing (ICCC ). IEEE; 2013. p. 352–7.
[89] Ali Khan MY, Saeed L, Khan SH, Saleem J. Design of a multi-input single-output DC-DC boost converter for micro grid application. In: 2019 international conference on engineering and emerging technologies, ICEET 2019. IEEE; 2019. p. 1–6.
[90] Moury S, Lam J, Srivastava V, Church R. A novel multi-input converter using soft-switched single-switch input modules with integrated power factor correction capability for hybrid renewable energy systems. In: IEEE applied power electronics conference and exposition (APEC). IEEE; 2016. p. 786–93.
[91] Zhao R, Kwasinski A. Multiple-input single ended primary inductor converter (SEPIC) converter for distributed generation applications. In: IEEE energy conversion congress and exposition. IEEE; 2009. p. 1847–54.
[92] Zhao R, Kwasinski A. Analysis of decentralized controller for multiple-input converters. In: Twenty-seventh annual IEEE applied power electronics conference and exposition (APEC). IEEE; 2012. p. 1853–60.
[93] Yu S, Zhao R, Kwasinski A. Design considerations of a multiple-input isolated single ended primary inductor converter (SEPIC) for distributed generation sources. In: IEEE energy conversion congress and exposition. IEEE; 2011. p. 3960–7.
[94] Haghighian SK, Tohidi S, Feyzi MR, Sabahi M. Design and analysis of a novel SEPIC-based multi-input DC/DC converter. IET Power Electron 2017;10: 1393–402.
[95] Sun Z, Bae S. Multiple-input soft-switching cuk converter. In: IEEE energy conversion congress and exposition (ECCE). IEEE; 2017. p. 2272–6.
[96] Moury S, Lam J. New soft-switched high frequency multi-input step-up/down converters for high voltage DC-distributed hybrid renewable systems. In: IEEE energy conversion congress and exposition (ECCE). IEEE; 2017. p. 5537–44.
[97] Wai R-J, Hong L-S. High-efficiency dual-input converter with high-voltage gain and internal charge function. IET Power Electron 2014;7:299–315.
[98] Dobbs BG, Chapman PL. A multiple-input DC-DC converter topology. IEEE Power Electron Lett 2003;1:6–9.
[99] Khaligh A, Cao J, Lee YJ. A multiple-input DC-DC converter topology. IEEE Trans Power Electron 2009;24:862–8.
[100] Yuan-mao Y, Cheng KWE. Multi-input voltage-summation converter based on switched-capacitor. IET Power Electron 2013;6:1909–16.
[101] Ye Y, Cheng KWE. Multi-port voltage-subtracting circuit based on resonant switched-capacitor. IET Power Electron 2012;5:693–701.

[102] Akar F, Kale M. A high voltage gain multi-input converter. In: 2nd international symposium on multidisciplinary studies and innovative technologies (ISMSIT). IEEE; 2018. p. 1–4.
[103] Khosravi M, Khaburi DA, Heshmatian S. Predictive control of multi-input switched-capacitor DC-DC converter with reduced switching frequency. In: 2017 8th power electronics, drive systems & technologies conference (PEDSTC). IEEE; 2017. p. 549–54.
[104] Mahmoodieh MES, Deihimi A. Battery-integrated multi-input step-up converter for sustainable hybrid energy supply. IET Power Electron 2019;12:777–89.
[105] Kardan F, Alizadeh R, Banaei MR. A new three input DC/DC converter for hybrid PV/FC/battery applications. IEEE J Emerg Sel Top Power Electron 2017;5: 1771–8.
[106] Banaei MR, Ardi H, Alizadeh R, Farakhor A. Non-isolated multi-input–single-output DC/DC converter for photovoltaic power generation systems. IET Power Electron 2014;7:2806–16.
[107] Azizi M, Mohamadian M, Beiranvand R. A new family of multi-input converters based on three switches leg. IEEE Trans Ind Electron 2016;63:6812–22.
[108] Wai R-J, Lin C-Y, Liaw J-J, Chang Y-R. Newly designed ZVS multi-input converter. IEEE Trans Ind Electron 2011;58:555–65.
[109] Wai R-J, Lin C-Y, Chen B-H. High-efficiency DC–DC converter with two input power sources. IEEE Trans Power Electron 2012;27:1862–75.
[110] Mohammadi P, Moghani JS. Double-input high-gain bidirectional DC-DC converter for hybrid energy storage systems in DC-micro grid. In: 9th annual international power electronics drive systems and technologies conference (PEDSTC). IEEE; 2018. p. 312–7.
[111] Feyzi MR, Niapour Mozaffari SAK, Nejabatkhah F, Danyali S, Feizi A. Brushless DC motor drive based on multi-input DC boost converter supplemented by hybrid PV/FC/battery power system. In: 2011 24th Canadian conference on electrical and computer engineering(CCECE). IEEE; 2011. p. 442–6.
[112] Ahrabi RR, Ardi H, Elmi M, Ajami A. A novel step-up multiinput DC-DC converter for hybrid electric vehicles application. IEEE Trans Power Electron 2017;32: 3549–61.
[113] Nejabatkhah F, Danyali S, Hosseini SH, Sabahi M, Niapour SM. Modeling and control of a new three-input dc-dc boost converter for hybrid PV/FC/battery power system. IEEE Trans Power Electron 2012;27:2309–24.
[114] Ghavidel BZ, Babaei E, Hosseini SH. An improved three-input dc-dc boost converter for hybrid PV/FC/battery and bidirectional load as backup system for smart home. In: 10th international power electronics, drive systems and technologies conference (PEDSTC). IEEE; 2019. p. 533–8.
[115] Balaji C, Dash SS, Hari N, Babu PC. A four port non-isolated multi input single output DC-DC converter fed induction motor. In: IEEE 6th international conference on renewable energy research and applications (ICRERA). IEEE; 2017. p. 631–7.
[116] Nahavandi A, Hagh MT, Sharifian MBB, Danyali S. A nonisolated multiinput multioutput DC-DC boost converter for electric vehicle applications. IEEE Trans Power Electron 2015;30:1818–35.
[117] Athikkal S, Guru Kumar G, Sundaramoorthy K, Sankar A. A non-isolated bridge-type DC-DC converter for hybrid energy source integration. IEEE Trans Ind Appl 2019;55:4033–43.
[118] Athikkal S, Kumar GG, Sundaramoorthy K, Sankar A. Performance analysis of novel bridge type dual input DC-DC converters. IEEE Access 2017;5:15340–53.
[119] Kumaravel S, Kumar GG, Veeranna K, Karthikeyan V. Novel non-isolated modified interleaved DC-DC converter to integrate ultracapacitor and battery sources for electric vehicle application. In: 2018 20th national power systems conference. NPSC); 2018. p. 1–6.
[120] Prabhala VAK, Fajri P, Gouribhatla VSP, Baddipadiga BP, Ferdowsi M. A DC-DC converter with high voltage gain and two input boost stages. IEEE Trans Power Electron 2016;31:4206–15.
[121] Hosseini SH, Mohseni P, Sabahi M. An extended high step-up multi-input DC-DC converter. In: 10th international conference on electrical and electronics engineering. ELECO); 2017. p. 285–9.
[122] Mohseni P, Hosseini SH, Sabahi M, Jalilzadeh T, Maalandish M. A new high step-up multi-input multi-output DC-DC converter. IEEE Trans Ind Electron 2019;66: 5197–208.
[123] Zhu B, Zeng Q, Vilathgamuwa DM, Li Y, She X. Non-isolated high-voltage gain dual-input DC/DC converter with a ZVT auxiliary circuit. IET Power Electron 2019;12:861–8.
[124] Varesi K, Ghandomi AA, Hosseini SH, Sabahi M, Babaei E. An improved structure for multi-input high step-up DC-DC converters. In: 8th power electronics, drive systems & technologies conference (PEDSTC). IEEE; 2017. p. 241–6.
[125] Varesi K, Hosseini SH, Sabahi M, Babaei E. Modular non-isolated multi-input high step-up dc–dc converter with reduced normalised voltage stress and component count. IET Power Electron 2018;11:1092–100.
[126] Varesi K, Hosseini SH, Sabahi M, Babaei E. A multi-port high step-Up DC-DC converter with reduced normalized voltage stress on switches/diodes. In: 9th annual power electronics, drives systems and technologies conference. PEDSTC); 2018. p. 1–6.
[127] Mohammadi S, Dezhbord M, Babalou M, Azizkandi ME, Hosseini SH. A new non-isolated multi-input DC-DC converter with high voltage gain and low average of normalized peak inverse voltage. In: 10th international power electronics, drive systems and technologies conference. PEDSTC); 2019. p. 515–20.
[128] Jabbari M, Dorcheh MS. Resonant multi-input/multi-output/bidirectional ZCS step-down DC-DC converter with systematic synthesis for point-to-point power routing. IEEE Trans Power Electron 2018;33:6024–32.
[129] Babaei E, Abbasi O. Structure for multi-input multi-output dc–dc boost converter. IET Power Electron 2016;9:9–19.
[130] Jafari M, Hunter G, Zhu JG. A new topology of multi-input multi-output buck-boost DC-DC converter for microgrid applications. In: IEEE international conference on power and energy (PECon). IEEE; 2012. p. 286–91.
[131] Gorji JG, Abbaszadeh K, Bagheroskouei F. A new two-input and multi-output interleaved DC-DC boost converter for satellites power system. In: 10th international power electronics, drive systems and technologies conference (PEDSTC). IEEE; 2019. p. 236–41.
[132] Saeed L, Khan MYA, Arif M, Majid A, Saleem J. A multiple-input multiple-output non-inverting non-isolated bidirectional buck/boost converter for storage application. In: International conference on computing, mathematics and engineering technologies (iCoMET). IEEE; 2018. p. 1–6.
[133] Khan MYA, Saeed L, Saleem J, Arif M, Majid A. A high gain multi-port bidirectional non-isolated DC-DC converter for renewable integration. In: International conference on computing, mathematics and engineering technologies. iCoMET; 2018. p. 1–6.
[134] Khan MA, Husain I, Sozer Y. A bi-directional DC-DC converter with overlapping input and output voltage ranges and vehicle to grid energy transfer capability. IEEE J Emerg Sel Top Power Electron 2014;2:507–16.